

**Use of Satellite Data to Improve the Physical Atmosphere in SIP Decision  
Making Models**

**Final Report**

Richard McNider  
Arastoo Pour-Biazar  
Earth System Science Center  
University of Alabama in Huntsville

William Crosson  
Universities Space Research Association  
National Space Science and Technology Center

Jon Pleim  
Atmospheric Modeling Division  
U.S. EPA National Environmental Research Laboratory

Aijun Xiu  
University of North Carolina

Under NASA Applications Program  
NASA-Ames Award No. NNA07CN20A

**Period of Performance: 01/15/06-12/15/09**

December 23, 2009

## Executive Summary

The purpose of this project was to employ satellite data into the State Implementation Plan (SIP) modeling process, in which emission reduction strategies are defined to reduce air pollution levels to meet National Ambient Air Quality Standards (NAAQS). Across the country tens of billions of dollars in emission controls depend on this modeling process. The focus of the project was to use satellite data to improve the simulation of the physical atmosphere in which emission reduction scenarios are evaluated. Errors in specification of atmospheric physical variables such as temperature, winds, photochemical production rates and mixing heights can alter the efficiency and efficacy of emission control strategies. A series of benchmark experiments were made to determine the impact of satellite data in the modeling system.

Techniques for using satellite data to specify photolysis rates in photochemical models were incorporated into models used by state governments in the SIP process. The technique was incorporated into EPA's Community Multi-scale Air Quality (CMAQ) System and was made part of EPA's December 2008 official release of CMAQ version 4.7 to the air quality community. Additionally, the State of Texas incorporated the technique into their CAMX SIP model. Clouds have a major impact on photolysis rates which are a first order parameter in determining photochemical production rates in models. Baseline runs under this activity showed that incorporating the satellite data improved the photolysis rates and changed ozone levels in the model by up to 70 ppb.

Additionally, techniques that used satellite data to improve temperature and mixing height calculations in the SIP model were tested in benchmark studies. The results showed that satellite adjustment in surface moisture and heat capacity improved the prediction of temperature compared both to high resolution satellite data and National Weather Service data. Comparisons of special aircraft mixed layer height predictions using satellite data showed that improved performance compared to the baseline case without satellite data.

## Table of Contents

Executive Summary .....	2
Table of Contents .....	3
List of Figures .....	4
List of Tables .....	6
List of Acronyms .....	7
I. Introduction .....	8
II. Definition of Problem .....	8
III. Description of Baseline System .....	9
IV. Enhancements to System .....	12
V. Evaluation Phase .....	17
VI. Validation and Verification Phase .....	18
VII. Benchmarking Phase .....	19
VIII. Transition of Products to the User Community .....	24
IX. Lessons Learned and Recommendations .....	25
X. References .....	27

## List of Figures

Figure 1. Example schematic of how satellite data are used to replace cloud model variables needed to make cloud adjustments to photolysis rates in the CMAQ system.

Figure 2. Example schematic of how satellite skin temperature tendencies are used to adjust soil moisture. Based on the difference in tendencies between the model and satellite during the morning period the surface moisture is adjusted using equation (6). Note that satellite temperatures are not directly assimilated but are used to adjust moisture.

Figure 3. Upper left: evening skin temperature tendency from the model using MM5 standard heat capacity values. Upper right: evening skin temperature tendencies observed by GOES. Lower left: default heat capacity values in the land use table used in MM5 for the 25 class USGS land use scheme. Lower right: derived heat capacity using equation (7) [from McNider *et al.* 2005].

Figure 4. Modeling domains for TexAQS2000 modeling episode.

Figure 5. Example of use of satellite albedo during the 2000 benchmark period. Upper left: land use classifications which are normally used to specify land surface parameters such as albedo. Upper right: albedo based on the land use classes. Lower panels: 30 day satellite derived albedo at two different times. While land use class specification of albedo captures the broad aspects of albedo they cannot capture the dynamic changes due to plant phenology.

Figure 6. Comparison of surface insolation where model clouds impact insolation values (upper left -control) with satellite derived insolation values (lower right – assimilation).

Figure 7. Left: climatological moisture values from the land use classifications used in the baseline run. Right: retrieved surface moisture using the satellite skin tendencies to adjust the baseline moisture.

Figure 8. Illustration of the impact of surface moisture assimilation on skin temperature differences between the baseline case and the case with satellite assimilation. Upper left: satellite observed surface skin temperature. Upper right: retrieved surface moisture using equation (6). Bottom left: predicted ground surface temperatures using the satellite retrieved surface moisture. Bottom right: default benchmark temperatures without satellite data.

Figure 9. Comparison of grid scale heat capacity values using the MM5 baseline method of land use classes with the satellite derived values using equation (7). Upper left: values from the land use classes. Upper right: heat capacity values as retrieved from the satellite technique.

Figure 10. The evolution of surface moisture and grid scale heat capacity during the 2000 benchmark period. Left: time evolution of the satellite retrieved surface moisture average over the whole 12km domain. Right: corresponding change in grid scale heat capacity.

Figure 11. Comparison of satellite skin temperatures and corresponding ground radiating temperatures in MM5 for a day during the 2000 experiment. Upper panel: 16:00 GOES skin temperature. Lower panels: ground radiating temperature for both the control benchmark run and the case where satellite insolation, satellite albedo, satellite derived surface moisture and satellite derived heat capacity were used in the model run.

Figure 12. Example of the use of satellite skin temperatures compared to model radiating ground temperatures as a model evaluation tool. Note that model performance without satellite assimilation degrades as finer resolution is employed.

Figure 13. Depiction of model bias as satellite data are added. The red line shows the control experiment without satellite data. Note in general daytime under-prediction of temperatures and nighttime over-prediction. Blue line gives bias after inclusion of satellite insolation, albedo and moisture adjustment is made. Increases in temperature change bias to positive (over-prediction).. Inclusion of heat capacity reduces the net bias.

Figure 14. Depiction of spatial model performance compared to NWA 2m air temperatures with and without satellite data. Top: mean bias with satellite (right) and without satellite data (left). Lower panel: same for root mean square error.

Figure 15. Top: boundary layer height or mixed layer height observations by the NOAA P3 aircraft. Lower left: model predicted boundary layer heights for the case without satellite data. Lower right: model predicted boundary layer heights with the added satellite data.

Figure 16. Top: differences in ozone between two CMAQ runs with and without use of satellite derived photolysis fields. Note the maximum differences exceed 50 ppb. Bottom: time series of ozone prediction from the model vs. observations at an EPA monitoring site in South Mississippi.

Figure 17. Comparisons of surface insolation with and without satellite data in the WRF model. Upper left: insolation values using WRF generated clouds. Upper right: solar insolation in WRF using GOES insolation values. Lower panel: differences in insolation values.

Figure 18. Comparison of model specific humidity show with NWS observed specific humidity (derived from dew point temperatures). The results show that the benchmark or control case (left panel) shows that the model is too moist. The case with the satellite adjustment (right panel) shows that the model has actually over-dried the atmosphere.

## **List of Tables**

Table 1 MM5 configuration for the 2000 modeling period.

Table 2 MM5 configuration for the 2006 modeling period.

## List of Acronyms

AMD	Atmospheric Modeling Division
CAA	Clean Air Act
CEM	Continuous Emissions Monitoring
CMAQ	Community Multiscale Air Quality
DMS	Decision Making System
EDAS	Eta-based 4-D Data Assimilation System
EOS	Earth Observing System
EPA	(US) Environmental Protection Agency
EGU	Electric Generating Units
FDDA	Four-Dimensional Data Assimilation
GHRC	Global Hydrology Resource Center
GOES	Geostationary Operational Environmental Satellites
GPGS	GOES Product Generation System
HPMS	Highway Performance Monitoring System
LST	Land Surface Temperature
LULC	Land Use/Land Cover
MM5	Mesoscale Model version 5
MODIS	Moderate Resolution Imaging Spectroradiometer
MSFC	Marshall Space Flight Center
NAAQS	National Ambient Air Quality Standards
NCAR	National Center for Atmospheric Research
NCEP	National Centers for Environmental Prediction
NERL	National Environmental Research Laboratory
NLCD	National Land Cover Data
NSSTC	National Space Science and Technology Center
NWS	National Weather Service
PM <sub>2.5</sub>	Particulate Matter with diameter less than 2.5 microns
RADM	Regional Acid Deposition Model
SIP	State Implementation Plan
SPoRT	Short-term Prediction Research and Transition Center
TexAQS2000	Texas Air Quality Study 2000
UAH	University of Alabama in Huntsville
USRA	Universities Space Research Association
WRF	Weather Research and Forecasting

## I. Introduction

In 2006, NASA's Applied Sciences Program funded the University of Alabama in Huntsville (UAH), in collaboration with the Universities Space Research Association (USRA), on a project entitled *Use of Satellite Data to Improve the Physical Atmosphere in SIP Decision Making Models*. The decision making system (DMS) used in this project was a coupled modeling system comprising a mesoscale meteorological model and a photochemical model. In various stages of the project, either the Mesoscale Model Version 5 (MM5) or the Weather Research and Forecasting (WRF) mesoscale model was used. MM5 is a mesoscale atmospheric model developed at Pennsylvania State University, while WRF is a fairly recent derivative of MM5. The air chemistry model used here is Community Multiscale Air Quality (CMAQ), developed by EPA. The coupled modeling system, described in more detail in section III, is typical of the SIP systems now used by states.

The project was conducted in partnership with U.S. Environmental Protection Agency (EPA)'s Atmospheric Modeling Division (AMD) at the National Environmental Research Laboratory (NERL) in Research Triangle Park, NC. AMD/NERL was the original designer and builder of CMAQ. This project resulted in the transfer of satellite assimilation and retrieval techniques developed over the last two decades under NASA sponsorship into the MM5/CMAQ system. The physical products used for data assimilation and model validation include:

- Surface albedo from Geostationary Operational Environmental Satellites (GOES)
- MODIS derived land surface emissivity
- GOES land surface temperature (LST)
- Heat capacity derived from GOES LST
- Insolation from GOES
- GOES satellite data (cloud top pressure, temperature and albedo) used to determine photolysis rates

The benchmarking phase of the project was based on testing MM5/CMAQ model performance with and without the satellite products. The model comparisons were made against standard National Weather Service (NWS) observations, the Texas Air Quality Study 2000 (TexAQS2000) special field program data set as well as GOES and Moderate Resolution Imaging Spectroradiometer (MODIS) satellite skin temperature products.

## II. Definition of Problem

The nation's air pollution control program under the Clean Air Act (CAA) is built around the development of State Implementation Plans (SIPs), which define specific emission reduction strategies for meeting the NAAQS. States usually identify time periods called "design days" in which observed air quality levels exceed the NAAQS by the largest margins. These periods are used to test whether sets of emission reductions will concomitantly reduce ambient air quality levels to meet the NAAQS. The evaluation process begins with a demonstration that the models are able to replicate the design day by reasonably simulating the observed air pollution levels. Next, the models must demonstrate that industry-specific emission reductions result in

compliance with the NAAQS. Without these demonstrations a SIP will not be approved. The cumulative costs of implementing individual SIP control strategies amount to billions of dollars for states and industry. The efficacy and efficiency of control strategies are a major consideration in determining whether they will be adopted by states and implemented by the affected industries without litigation. Comparison of model performance to physical and air quality observations is a major factor in building the confidence of the regulating and regulated communities.

This project focused on models used to estimate concentrations of ozone and fine particulate matter (PM<sub>2.5</sub>) - two of the most complex and pervasive air pollutants in terms of non-attainment of NAAQS. In the past, simple proportional rollback models were used to test strategies and demonstrate compliance. Today all states use full photochemical models for this purpose. There are several EPA-approved decision-making models. These models have a number of characteristics in common. All have an emissions processor that converts emission inventory and ancillary data to gridded emissions. All have a meteorological or physical model that produces wind fields, temperature, and turbulent information. These models are often special forms of general mesoscale models such as MM5 that can carry out continuous data assimilation. The models also have a photochemical transformation and transport component. The output from the meteorological model is used in both the emissions processor and the photochemical transport model.

The meteorological and chemical models are run for the design days including a preceding spin-up period. The meteorological model is used to re-create atmosphere properties such as temperature, which impacts chemical kinetics and emissions, wind speed and wind direction, and mixing heights. The chemical model is used to simulate air quality and to test whether emission reductions will reduce air pollution levels below the NAAQS. Currently MM5 is one of the most widely-used meteorological models in SIP and air quality research. The atmosphere simulated by the model is important not only because it is needed to make photochemical predictions but also because any errors it contains can alter the impact of controls.

### **III. Description of Baseline System**

There are several different modeling systems that have been used in the SIP modeling process. These have been developed by states, private industry and with support by the U.S. EPA. Examples of these models are CAMX, UAM and RADM. In general these modeling systems have three major components:

- (1) a meteorological model that attempts to re-create the physical atmosphere for the design period;
- (2) an emissions processor that uses inventories of point source emissions, transportation information, land use data and meteorological information to provide gridded and temporal information on anthropogenic and natural emissions;
- (3) a chemical transport model that calculates transport, transformation and deposition of dozens of from chemical species.

EPA itself developed an air quality modeling system at the National Environmental Research Laboratory (NERL) in North Carolina. This system, referred to as CMAQ, was designed to be a community model in that it could be run and modified by the air quality community. Because of its openness and documentation in the air quality community this was the model chosen for this NASA Applications Benchmark activity. In fact, as mentioned above the lead developers of this model at NERL were one of the applied partners in this activity.

**Meteorological Model:** The meteorological model most widely used in CMAQ is the MM5 (Grell et al. 1994; Dudhia and Bresch 2002) which was developed from a Pennsylvania State University mesoscale model in the early 1970's (Anthes and Warner 1978) and is used to simulate local and synoptic scale meteorological conditions prevalent during the period of interest. The MM series of models was adopted by the National Center for Atmospheric Research (NCAR) as a community model. Since inception, the MM series of models culminating with MM5 has undergone many changes designed to broaden its usage. These include (1) a multiple-nest capability; (2) non-hydrostatic dynamics that allow the model to be used at a scale of approximately 4 km; (3) multi-tasking capability on shared and distributed-memory machines; (4) four-dimensional data assimilation (FDDA) capability, and (5) multiple physics options (<http://box.mmm.ucar.edu/mm5>). Required data inputs include topography and land cover/land use (LULC) data, gridded atmospheric fields of sea-level pressure, wind, temperature, relative humidity and geopotential height at defined pressure levels, and observation data including soundings and surface reports. LULC is used as input directly to MM5 to provide surface boundary conditions such as albedo, soil moisture availability, surface roughness and canopy height. It is a critical element in MM5 because of its influence on surface fluxes and consequently boundary layer states.

Like any other prognostic meteorological model, MM5 requires a significant amount of terrestrial (i.e., topography, LULC) and atmospheric data (e.g., gridded analysis fields that include at a minimum sea level pressure, wind, temperature, relative humidity, and observations that contain soundings and surface reports). In this modeling project surface elevation, LULC, soil type, and other terrestrial datasets from United States Geological Survey (USGS); NCEP ETA gridded analysis data at 40-km resolution archived at 3-hour intervals available at <http://dss.ucar.edu/datasets/ds609.2>; surface (land and ship) and upper air observational data archived at 3 and 6-hour intervals available at <http://dss.ucar.edu/datasets/ds464.0>; and hourly surface observations for over 1,000 stations in U.S. and Canada available at <http://dss.ucar.edu/datasets/ds472.0> were utilized.

While MM5 has been the preferred meteorological model for use with the CMAQ system, the development and support of MM5 as a community model has been discontinued. In its place is the Weather Research and Forecast (WRF) model which is a joint undertaking of NOAA and NCAR. While it may take several years for the WRF model to be embraced by the air quality regulatory community, WRF is now being run by EPA NERL in test modes. Thus, we have started a transition of the satellite tools to the WRF model platform. Some testing of the satellite techniques were made with the WRF model.

**Chemical Transport Model:** The chemical transport model used in the system was developed as a new modeling system by EPA but some of its structure evolved from earlier models. It has been extensively used by EPA and the research community an extensively and contains state-of-the-science parameterization of atmospheric processes affecting transport, transformation, and deposition of ozone and other pollutants. CMAQ incorporates outputs from MM5 and SMOKE

modeling systems and other data sources through special processors to create gridded emissions data. Remotely-sensed input data include the National Land Cover Data (NLCD). Large-scale meteorological data obtained from the National Centers for Environmental Prediction (NCEP) were used as lateral boundary conditions in MM5. Data sets used by these models include: BELD3; traffic volume data from the Highway Performance Monitoring System (HPMS) of the U.S. DOT; and Continuous Emissions Monitoring (CEM) data for the Electric Generating Units (EGU) available from the U.S. EPA.

### ***Shortcomings of the baseline system***

The intent of this project was to improve the characterization of the physical atmosphere and the land surface in a coupled mesoscale/air quality model, with the ultimate goal of improving air quality simulations used in the SIP modeling process. One of the major sources of error in the SIP simulation system is the model prediction of clouds including their position in time and space and their radiative characteristics (McNider et al 1995). The erroneous position of clouds impacts surface insolation which in turn impacts temperatures and mixing heights. Clouds also have a major impact on photochemical reaction rates.

A second major source of error in SIP simulations is the proper specification of surface moisture, surface heat capacity and surface albedo. These parameters impact the rate at which the surface warms and cools. Surface albedo (surface reflection) impacts the amount of sun's energy which is available to heat the surface. Surface moisture largely controls the rate at which the land surface heats up in the morning (Wetzel 1984). The grid scale heat capacity controls the rate at which the surface loses heat at night (Carlson 1986). None of these parameters is directly observable from surface information. Initial guesses of these parameters are based on climatology and values associated with land classification schemes. However, errors in their specification can lead to errors in surface temperature which in turn impact mixed layer heights, winds and chemical kinetic rates.

With respect to the land surface properties that were assimilated in this project, both surface albedo and heat capacity are typically (and in the baseline model configuration) specified as functions of LULC type. This practice obviously introduces errors as it does not take into account vegetation state or phenology, soil moisture, or the actual mix of land cover types within a model grid cell. While specification of heat capacity is relatively straightforward for single composition objects such as water, stone, concrete etc., the specification of heat capacity on a 4 km or 12 km grid where the surface is composed of everything from buildings and paved areas to grass, trees and small bodies of water is extremely difficult. This is especially true in the highly heterogeneous urban and suburban environments.

A major factor in air quality modeling is the accurate simulation of photodissociation reaction rates (or photolysis rates) for chemical species in the atmosphere (Pour-Biazar et al. 2007). These rates depend on the solar radiation flux profiles and the properties of the molecule undergoing photodissociation. Since clouds significantly alter the solar radiation in the wavelengths affecting photolysis rates, they have major impacts on photochemistry. Thus, any errors in predicting cloud amount and optical depth seriously diminish the skill with which a photochemical model can predict generation of air pollutants. Many previous studies (Collins et al. 2000; Liao et al. 1999; Jacobson 1998; Dickerson et al. 1997) have shown that clouds

substantially modify the photolysis rate via absorption and attenuation of incoming solar radiation.

CMAQ uses a two-step approach for calculating photolysis rates, similar to that used in the Regional Acid Deposition Model (RADM; Chang et al. 1987). In short, the first step, performed in pre-processing, uses a radiative transfer model to calculate clear-sky photolysis rates, and then these rates are corrected based on simulated cloud cover for each grid cell and time step. There are two major concerns with this approach as far as cloud correction is concerned (Pour-Biazar et al. 2007). First, estimation of cloud transmissivity in models is highly parameterized and, therefore, introduces a large uncertainty. Second and most important, the cloud information is provided to the air quality model by the mesoscale atmospheric model, which has difficulty with the spatial and temporal placement of clouds.

## **IV. Enhancements to System**

### ***GOES surface albedo and insolation***

The ground surface albedo and insolation are critical parameters in the surface energy budget, which controls fluxes, temperature and boundary layer characteristics. Under this activity satellite measures of albedo and insolation are used instead of standard model values. The Infrared Measurement and Processing Group (hereinafter IR Group) at the National Space Science and Technology Center (NSSTC) performed the satellite retrievals for this study. Currently, the IR group uses GOES Product Generation System (GPGS) to provide routine real-time retrievals of skin temperature, total precipitable water, cloud top pressure, cloud albedo, surface albedo and surface insolation for the use of meteorological and air quality models (Haines et al., 2004).

The algorithm used for the retrieval of surface albedo and insolation is an implementation of the methods of Gautier et al. (1980) and improvements thereof from Diak and Gautier (1983); details are given in Pour-Biazar et al. (2007). The method uses the information from GOES Imager visible channel (.52-.72  $\mu\text{m}$ ) at 1-km resolution, and employs a clear and a cloudy atmosphere to explain the observed upwelling radiant energy. The model applies the effects of Rayleigh scattering (Coulson 1959; Allen 1963), ozone absorption (Lacis and Hansen 1974), water vapor absorption (Paltridge 1973), cloud absorption, and cloud reflection. Water vapor absorption is assumed to be negligible in the surface albedo calculations, but is accounted for when applying the total solar flux in the surface insolation calculation. Total column water vapor was assumed to be 25 mm and adjusted for solar zenith angle. Cloud absorption was assumed to be a constant 7% of the incident flux at the top of the cloud (Diak and Gautier 1983).

The surface albedo is calculated using the clear-sky composite image. For the current study, a 20-day composite centered on the case study period was used to generate the clear-sky composite image. The composite represents the minimum albedo value for each pixel for a given hour of the day. Assuming that for any given hour of the day (for the entire 20-day period) each pixel experiences clear skies at least once, the minimum value represents the clear-sky value for that pixel. This formulation also assumes that the visible channel surface albedo does not vary significantly within the time period of the composite.

Surface insolation is calculated as the sum of solar radiation incident at the surface from both direct and diffuse sources and also includes the effect of attenuation by clouds. For the clear-sky case, the incident short-wave radiation at the surface is the sum of 1) the incident solar flux that is attenuated by Rayleigh scattering, ozone and water vapor absorption, and 2) the surface reflected flux scattered back to the surface by Rayleigh scattering. With known surface albedo and estimated absorption and scattering, the surface insolation is calculated directly.

For the cloudy-sky case, the radiance observed by the satellite is assumed to be a function of the incident solar flux undergoing several processes. The satellite-observed radiant energy is the sum of atmospheric backscatter, reflection of the incident solar flux from the cloud surface, backscatter within the cloud by Rayleigh scattering, and the surface reflection that reaches the satellite after attenuation. Since the radiance at the satellite, the surface albedo and the scattering and absorption are known or estimated, the radiation formulation can then be solved for the cloud albedo. In practice, the algorithm calculates a surface insolation using both the clear-sky and cloudy-sky formulations for a given scene. If the cloudy-sky calculation is greater than or equal to the clear-sky value, then the clear-sky value is used and the scene is assumed clear. This is consistent with the cloud albedo being near zero for clear-sky conditions. Since the effect of cloud albedo dominates in the insolation calculation, uncertainties in cloud thickness have shown to produce only small effects on the surface insolation calculation.

### ***MODIS emissivity in model surface energy budget and in GOES Land Surface Temperatures***

In the surface energy budget of MM5 an outgoing radiation term appears. This longwave radiation term,  $LW\uparrow$ , expresses the radiational loss of energy from the surface. It is represented by the Stefan-Boltzman equation, in which  $\sigma$  is the Stefan-Boltzman constant and  $\epsilon$  is the surface emissivity:

$$LW\uparrow = \epsilon\sigma T_s^4 \quad (1)$$

In most models the emissivity is general assumed to be 1.0. In actuality, emissivity is a function of the land surface and can vary from 0.93 to 1.00. However, accurate values of emissivity of grid scale surfaces are hard to determine.

The MODIS instruments on NASA's Aqua and Terra satellites have spectral channels in the longwave infrared window region that are similar to those found on the instruments of the GOES satellites with resolutions similar to those planned for the Advanced Baseline Imager of the GOES-R series of satellites. One of the physical parameters produced by the EOS MODIS land surface team that could be useful in the surface energy budget specification is the surface emissivity. Improved specification of surface emissivity would also improve the retrieval of a skin temperature from GOES radiances. It would also facilitate the use of GOES skin temperatures to evaluate model skin temperatures by enabling apples to apples comparison since common emissivity would be used in the model and GOES temperatures.

Under this activity we examined whether MODIS emissivities can be used in the model and in GOES skin temperature retrievals.

### ***GOES cloud properties for photolysis rates– cloud top pressure and broadband transmittance***

Cloud properties such as cloud top, cloud bottom and cloud transmittance are needed in calculating cloud impacts on photolysis rates. In this activity satellite cloud properties were used instead of model values. Cloud albedo is a by-product of the insolation calculations above. Since the sum of cloud albedo ( $A_c$ ), cloud absorption ( $a_c$ ), and cloud transmittance is unity, then the broadband cloud transmittance,  $tr_c$ , is calculated as:

$$tr_c = 1 - (A_c + a_c) \quad (2)$$

The other needed vital information for the cloud correction is the cloud-top height. A cloud-top pressure was assigned to each cloudy pixel. The GOES 11- $\mu\text{m}$  window channel (of either the Imager or the Sounder) brightness temperature was used for this purpose. Clouds were assumed to be uniform in coverage and height over the GOES pixel. The brightness temperature for each cloudy pixel was referenced to the corresponding thermodynamic profile for the closest model grid.

The cloud-top pressure assignment is similar to that developed by Fritz and Winston (1962) and applied by Jedlovec et al. (2000). Log-linear interpolation was used between model vertical pressure levels to assign a corresponding cloud-top pressure.

The approach works well for opaque clouds where the cloud emissivity is close to unity and satellite-observed emission comes primarily from the cloud top. Typical pressure assignment errors are on the order of 25–50 mb. For non-opaque clouds such as thin cirrus, emission from below the clouds is detected by the satellite and cannot be separated from cloud emission without knowledge of the cloud emissivity. The bias would be greatest for low clouds. For air quality applications, since the focus is on the boundary layer, the error in the cloud-top pressure for opaque clouds does not pose a significant problem. Furthermore, in our technique the cloud-top height is only used for determination of the atmospheric layer in which photolysis rates are being interpolated, and does not impact the correction made to the photolysis rates within the boundary layer (as the transmittance is estimated directly from the satellite observations). In addition, the determination of cloud top in the model is limited by the vertical resolution of the model, which usually is too coarse in the free troposphere. For non-opaque clouds, cloud transmissivity is large and therefore the modifications to photolysis rates are small and thus the impact of the error in the cloud top height is further reduced. For low transparent clouds with unrealistic cloud top pressure, we allow for a thin cloud above the cloud base (one model layer thick).

### ***GOES-derived surface moisture from land surface tendencies***

Early in the development of boundary layer mesoscale models (Deardorff 1978; Wetzel 1978; McCumber and Pielke 1981; Zhang and Anthes 1982) and later in global scale models (Dickinson 1984; Sellers et al. 1986) it was recognized that the correct specification and partitioning of surface fluxes were critical to the accurate characterization of boundary layer behavior. In air quality simulations these boundary layer processes control mixing heights (impacting pollutant concentrations), temperatures (controlling thermal decomposition of PAN and other organic nitrates) and photolysis rates. As mentioned above surface moisture is not a standard observable. It depends on antecedent precipitation, soil water holding characteristics, and vegetative state which impacts evapotranspiration and can often change dramatically over

time and space due variation in these surface attributes. Because of the importance of the surface energy budget and uncertainties in its implementation within models, we and other investigators have attempted to develop techniques to use satellite information to improve the fidelity of the land-surface models (Price 1982; Carlson et al. 1981; Wetzel et al. 1984; McNider et al. 1994; Gilles and Carlson 1995; McNider et al. 1995; Jiang and Islam 1999).

A prognostic equation for the surface skin temperature, based on the surface energy budget, can be written in the following form (Wetzel 1984; Pielke et al. 1991; Smirnova 1997),

$$C_b \left( \frac{dT_G}{dt} \right) = (R_N + H + G) + E \quad (3)$$

where  $dT_G/dt$  is the rate of change of the LST,  $C_b$  the surface heat capacity,  $R_N$  is the net radiation (including incident shortwave, incoming atmospheric longwave, and outgoing longwave),  $H$  is the sensible heat flux,  $G$  is the soil heat flux, and  $E$  is the latent heat flux.

In the application of such an energy budget in a regional model, either separate budgets must be developed for vegetative canopies (perhaps further decomposed into deep rooted and shallow rooted vegetation), bare soil and standing water (McCumber and Pielke 1981; Smirnova 1997). Or, a composite surface must be formed which reflects the aggregate effects of these distinct components (Wetzel et al. 1984). Under the present activity we employed a simple composite surface because it allows analytical inversion to retrieve surface moisture and heat capacity. Additionally, the use of a single composite surface allows the natural averaging of the IR pixel to characterize the surface.

McNider et al. (1994), hereafter McN94, described a procedure that takes a practical approach towards assimilating LST by recognizing that adjustments in this parameter must be consistent with other components of the surface energy budget. The technique requires the use of GOES derived IR LST *tendencies* and GOES derived net solar radiation over the time period of interest. It is based upon adjusting the model's bulk moisture availability so that the model's *rate of change* of LST agrees more closely with that observed from the satellite. Therefore, the simulated latent heat flux, which is highly correlated with surface moisture availability during this time period, is adjusted based upon differences between the modeled and satellite-derived LST tendencies.

Following McN94, we first define the surface energy budgets for the model and satellite as in (1) by assigning subscripts  $m$  and  $s$  to all terms, respectively. Since we are now considering a composite surface representing the characteristics of vegetation, soil etc. rather than bare soil,  $C_b$  is no longer simply a heat capacity. It is more like a combination of heat capacity and thermal transfer and as a result represents a resistance to forcing (see McNider et al., 2005). Next, we invoke the critical assumption that all of the terms in the model's surface energy budget are the same as for the actual energy budget observed by the satellite except for the latent energy term,  $E$ . This is consistent with the ideas discussed above that we know the least about evapotranspiration and that in the mid-morning the energy budget is most sensitive to moisture availability (Wetzel et al., 1984). With this assumption we take the difference of the surface energy budgets for the model and satellite to obtain:

$$E_s = C_b \left[ \left( \frac{dT_G}{dt} \right)_s - \left( \frac{dT_G}{dt} \right)_m \right] + E_m \quad (4)$$

where  $(dT_G/dt)_s$  is calculated from hourly GOES-derived LST products retrieved at model grid points.

The way in which the moisture flux is adjusted within the model is dependent upon the flux formulation used. In McN94, the surface specific humidity was analytically recovered from similarity theory using this satellite-inferred evapotranspiration ( $E_s$ ). In MM5, surface specific humidity is not a prognostic variable. Therefore, we adjust what is called the moisture availability parameter ( $M$ ) which represents the *fraction* of possible evaporation for a saturated surface (equal to 1 over open water and 0 over a non-evaporating surface). The latent heat flux in the Blackadar boundary layer scheme in MM5 (Blackadar 1979; Zhang and Anthes 1982) is given by:

$$E_m = \frac{M \rho (q_{sat}(T_g) - q_a) k u_*}{\ln \left( \frac{k u_* z_a}{k_a} + \frac{z_a}{z_l} \right) - \varphi_h}, \quad (5)$$

where  $q_{sat}(T_g)$  is the saturation mixing ratio of the surface,  $q_a$  is the mixing ratio of the air immediately above the surface,  $k$  is the von Karman constant,  $u_*$  is the frictional velocity,  $z_a$  the height of the lowest model layer,  $z_l$  the depth of the molecular layer,  $k_a$  is a background molecular diffusivity, and  $\varphi_h$  is a non-dimensional stability parameter for heat and water vapor. To obtain the satellite-inferred moisture availability, we solve (5) for  $M$  using the satellite-inferred latent flux as derived from (4) and get the satellite inferred moisture availability

$$M_s = E_s \frac{\ln \left( \frac{k u_* z_a}{k_a} + \frac{z_a}{z_l} \right) - \varphi_h}{\rho k u_* (q_{sfc}(T_g) - q_a)}. \quad (6)$$

In addition to the recovery of moisture availability, the GOES derived net solar radiation is also assimilated into the model's surface energy budget via direct insertion.

This assimilation technique has been shown in case study tests and in a semi-operational environment to improve surface energy budget performance (Lapenta et al. 1999). Diak and Whipple (1995) also showed that LST tendencies from GOES could be used to estimate the partitioning of latent and sensible fluxes.

Figure 2 shows a schematic of how the model tendencies are adjusted in the morning time frame. This technique was used in the baseline simulations given below to determine any improvement to surface temperature predictions by adjusting the surface moisture availability

### ***GOES-derived heat capacity from LST***

Wetzel (1984) and Carlson (1986) showed in sensitivity studies that LST tendencies were most sensitive to surface moisture in the mid-morning time frame, but were most sensitive to

thermal inertia during the evening. In this project we utilized the approach taken by McNider et al. (2005), in which the evening LST tendencies are used to recover the surface heat capacity.

Consider that the model bulk heat capacity ( $C_{bm}$ ) may be different from what can be retrieved from satellite observations ( $C_{bs}$ ). This means that use of  $C_{bs}$  in the surface energy budget (equation 3) will yield the observed skin temperature tendency. We assume that the moisture availability has been correctly specified (or surface evaporation is negligible late in the day when plant stomata have closed), and there is negligible difference in net radiation, sensible, latent, and soil heat fluxes. Then we can subtract the model and satellite energy budget equations and solve for  $C_{bs}$  to get:

$$C_{bs} = C_{bm} \left( \frac{dT_G}{dt} \right)_m / \left( \frac{dT_G}{dt} \right)_s \quad (7)$$

The initial value for the model  $C_{bm}$  would be determined in the normal fashion via a simple lookup table. The new  $C_{bs}$  would be subsequently used as the model value.

The retrieval was tested in a case study mode and reported in McNider et al 2005. Figure 3 from that study shows the evening temperature tendencies in the MM5 using the default land use scheme -  $\left( \frac{dT_G}{dt} \right)_m$  and the corresponding evening tendencies as observed by GOES -  $\left( \frac{dT_G}{dt} \right)_s$ . As can be seen there is considerable differences in the rate at which the land loses energy. Over agricultural land declines are steep (e.g. along the Delta region of Mississippi). The rate of change is much less over heavily vegetated surfaces or water. The altered or retrieved heat capacities are given in the figure compared to the default land use classification values.

In the baseline studies given below this methodology was incorporated to determine if temperature predictions could be improved over the baseline simulations.

## V. Evaluation Phase

Enhancements were made to the DMS in two categories – modeled surface properties and cloud properties in MM5, the cloud properties were also used in the CMAQ model to calculate photolysis rates. For successful integration into the modeling system, data obtained from remote sensing or other platforms must meet a set of requirements related to spatial, temporal and accuracy characteristics of the data. These requirements are dictated primarily by the configuration of the modeling system. Because assimilation in this study was performed on the 4 km grids, a requirement for all data being assimilated was that they be available at 4 km or finer grid spacing.

Surface albedo exhibits a diurnal pattern but only small day-to-day variations. Albedo of a vegetated surface changes slowly due to the phenology, density and water stress of the canopy. If vegetation coverage is not complete, increases in soil moisture cause decreases in surface albedo. Based on these characteristics, the temporal requirement for albedo data is monthly representations of the diurnal albedo pattern. The accuracy requirement for albedo is  $\pm 0.05$ .

Surface insolation varies continuously due to changes in the solar zenith angle, cloud cover and atmospheric attenuation. Thus, hourly estimates of insolation with an accuracy of  $\pm 50 \text{ W/m}^2$  are required in the modeling system. A further requirement is that spatial and temporal variations in surface insolation are consistent with the corresponding variations in surface albedo.

Heat capacity of a mixed vegetation/soil surface is an effective value representing the contributions of the various elements. It depends on the amount and type of vegetation, soil type, and soil moisture. Temporal changes are generally slow, reflecting vegetation growth and senescence. However, large changes in soil moisture will cause correspondingly large changes in heat capacity. The most rapid changes in soil moisture are due to heavy rainfall. Thus, the required temporal resolution of heat capacity estimates is once per day. The heat capacity of the slab is actually a model heuristic and is not a direct physical variable. Since it acts in changing the slope in both morning and evening times, relative errors of more than 10% can negatively impact the retrieval of moisture or impact temperature predictions. Thus, the required relative accuracy of heat capacity is approximately 10%.

Cloud-top pressure, temperature and albedo are needed on an hourly basis, based on the time constant of clouds. Estimates are needed with the following accuracies:  $\pm 50 \text{ mb}$  for pressure,  $\pm 5 \text{ K}$  for temperature and  $\pm 0.05$  for albedo.

## **VI. Validation and Verification Phase**

The satellite based methods described above to improve specification of surface moisture appear to directly address issues that SIP modelers have had in the past with uncertain specification of surface moisture. As an example, in past air quality studies surface moisture availability has been used as a tuning factor to improve model predictions of boundary layer heights. However, such adjustments are often made over the entire model domain based on one or two point measurements of boundary layer height or limited numbers of surface temperature. The satellite skin temperature data at a horizontal resolution of order 4 km data appears to be an objective way of making the moisture adjustment using much more spatial information than has been available to SIP modelers in the past. The description and testing of the techniques have appeared in the literature (McNider et al. 1994, McNider 1998, McNider et al. 2005) and tested in several settings.

As indicated above the meteorological model's inability to place clouds at the right place and time as often been the weakest point in the modeling system. Yet, clouds through their impact on temperatures, mixed layer heights and photolysis rates directly impact air pollution precursor concentrations and photochemical production. While satellites have had limited success in being able to provide direct measures of air pollutants, satellites provide an excellent depiction of cloud location and radiative properties. Thus, the use of satellite derived clouds in place of model clouds has the potential to greatly increase the realism of SIP modeling events. These techniques have also appeared in the literature (McNider et al. 1995, McNider et al. 1998 and Pour-Biazar 2007).

The benchmarking studies discussed below make a natural transition from the research activities to application in real air quality simulations.

## VII. Benchmarking Phase

In this benchmarking section we will compare the DMS in its baseline mode without satellite data enhancements with DMS simulations including the enhancements. These benchmarking cases were run in conjunction with EPA NERL. In some cases we will provide simple depictions with and without the satellite data. In others we will compare the results of the DMS with and without satellite data to observations. In some cases the figures denoted control (CNTRL) represent the baseline case without satellite data. The DMS results with satellite enhancements are referred to as “satellite” or “with satellite” or “Assimilation”

Two main simulation periods were studied. The first was for the TEXAQS2000 data period from August 23 through September 1, 2000, which coincides with Texas Air Quality Study 2000. A second period was July 1 –September 30, 2006.

Modeling simulations were conducted on a base 36-km resolution grid that spans over the continental U.S. A Lambert Conformal map projection with origin at 40N and 97W and true latitudes at 33N and 45N were employed. The grid has 164 cells in the east-west and 128 cells in the north-south direction. Nested grids of 12 km and 4 km were used in the simulations. The top of the modeling grid has been fixed at 50 mb. It has 39 vertical layers of varying thickness. To avoid artificial numerical mixing near the top of the model, vertical layers are adjusted near the tropopause by increasing the number of layers in the upper troposphere/lower stratosphere. This is important as the ozone vertical gradient is the highest at the tropopause.

**2000 Simulation Period:** The 2000 study period coincided with the TEXAQS2000 intensive field study period so that the 2000 period is sometimes referred to as TEXAQS2000. The control MM5 simulations were performed for four domains from 108-km grid spacing that covered the entire continental United States, to 4-km grid spacing that covered Houston/Galveston Bay area with a ratio of 1/3 nesting (Figure 4). The model extended to 43 layers vertically from surface to a height of about 20-km (top pressure of 50 mb). The model was configured to use FDDA gridded nudging, no observational nudging, Dudhia simple ice moisture scheme using look-up tables for moist physics, Grell convective parameterization for all domains except 4 km in which no cumulus parameterization was used, Medium Range Forecast (MRF) PBL scheme, RRTM radiation scheme, shallow convection scheme, and 5-layer soil model. Grell cumulus parameterization has proven to be useful for smaller grid sizes (10-30 km). It tends to allow a balance between resolved scale rainfall and convective rainfall (Grell et al. 1991; Grell et al. 1994.)

For moisture availability adjustments the assimilation period is between 7:00 and 9:30 AM local time. Satellite retrieved insolation is assimilated for the entire daytime period. For the heat capacity adjustment satellite skin temperature retrievals from 15:00 to 18:00 local time was used.

**2006 Simulation Period:** Modeling simulations were conducted using MM5 version 3.7. Data processing was performed in six-day segments beginning July 1 and ending October 3<sup>rd</sup>. The

NCEP Eta-based 4-D Data Assimilation System (EDAS) analyses were utilized for these simulations (Eta is one of NCEP's mesoscale numerical weather prediction models and the name "Eta" derives from the model's vertical coordinate known as the "eta" or "step-mountain" coordinate). The NCEP ETA gridded analyses data were first processed through the program PREGRID and mapped onto the 36-km domain via the REGRIDDER. Surface, ship and upper air data are incorporated within the analyses fields with the help of the program LITTLE\_R. Finally, INTERPF is used to interpolate pressure level fields generated by LITTLE\_R onto MM5 sigma coordinates.

MM5 model configuration, presented in Table 1, for the 2000 case and Table 2 for the 2006 study was determined through past experience and through a brief literature review (Brewer et al. 2007; Kembal et al. 2005) of recent modeling projects that have been undertaken in support of air quality management activities.

Table 1. MM5 configuration for the 2000 modeling period.

<b>Physics options</b>	
Nesting Type	One-way
Numerical Time Step	150 sec for 108-km to 10 sec for 4-km domain
Cumulus parameterization	Grell
PBL scheme	MRF
Microphysics	Dudhia simple ice
Radiation scheme	RRTM scheme
Land Surface scheme	5-layer soil model
Shallow Convection	yes
Observation nudging	None
3-D Grid analysis nudging	Yes
3-D Grid analysis nudging time interval	3-hour
3-D Grid analysis nudging co-efficient	$GU=2.5 \times 10^{-4}$ , $GV=2.5 \times 10^{-4}$ , $GT=2.5 \times 10^{-4}$ , $GQ=1.0 \times 10^{-5}$
Surface Analysis nudging	No
Surface Analysis nudging time interval	3-hour

Table 2. MM5 configuration for the 2006 modeling period.

<b>Physics options</b>	
Nesting Type	One-way
Numerical Time Step	90 sec
Cumulus parameterization	Grell
PBL scheme	MRF
Microphysics	Reisner 1
Radiation scheme	RRTM scheme
Land Surface scheme	Noah-LSM
Shallow Convection	yes
Observation nudging	None

3-D Grid analysis nudging	Yes
3-D Grid analysis nudging time interval	3-hour
3-D Grid analysis nudging co-efficient	GU=2.5x10 <sup>-4</sup> , GV=2.5x10 <sup>-4</sup> , GT=2.5x10 <sup>-4</sup> , GQ=1.0x10 <sup>-5</sup>
Surface Analysis nudging	Yes
Surface Analysis nudging time interval	3-hour
Surface Analysis nudging co-efficient	GU=2.5x10 <sup>-4</sup> , GV=2.5x10 <sup>-4</sup>

### ***Role of satellite albedo***

Figure 5 shows the difference in surface albedo using the standard land use classification methods and that from the satellite. While the land use classifications capture the broad features of the variation in surface albedo (in part because they include satellite inputs) they cannot capture the dynamics of plant phenological changes over the growing season and other short-term changes in surfaces such as tilling of land.

The surface albedo has two roles in the DMS. First, the surface albedo impacts the surface energy budget and ultimately temperature and mixing heights. It also impacts photochemistry since reflected visible light can greatly enhance photolysis rates over light surfaces. Since we jointly included the surface albedo with surface insolation we cannot distinguish in these baseline runs the impact of albedo alone.

### ***Role of surface insolation***

Surface insolation is the major driver of surface heat fluxes and directly impacts temperatures. It also ultimately impacts boundary layer heights and mesoscale circulations such as sea breezes. Figure 6 shows the difference in insolation for the 2000 benchmark period between the default insolation as computed in MM5 using model clouds and the insolation derived from the satellite. Note particularly the north-south oriented heavy cloud over East Texas. The satellite shows a much weaker cloud system to the west and elongated more in a SW-NE orientation. Such differences in cloud cover can make significant differences in temperature. The two bottom panels of figure 7 (discussed in the next section) show how the erroneous clouds impact surface temperatures.

### ***Impact of satellite retrieved surface moisture***

During the TEXAQS2000 period, Texas modeling efforts carried out by Texas A&M showed that the default MM5 system drastically under-predicted surface temperatures. Thus, a manual adjustment was made to decrease moisture across the Texas domain. This then makes an interesting case to see whether the satellite technique of using skin temperature tendencies can correct the moisture in a spatially accurate manner. The baseline DMS (the MM5) was run in a standard mode using the moisture in the standard land use classifications. Figure 7 (upper left panel) shows the default moisture values used in the benchmark or control run without use of the satellite data. The upper right panel show the surface moisture availability retrieved from the satellite technique. As can be seen the surface is much drier and is consistent with the manual adjustment made by Texas A&M.

As mentioned above the available surface moisture is critical to how fast temperatures rise in the morning. Figure 8 shows the impact on afternoon temperatures of drying the surface based on the satellite retrieved moisture. The upper left panel shows GOES satellite observed skin temperatures at 16:00 local time. The lower right panel shows the model predicted ground temperatures using the model default land use class climatological values of surface moisture. As can be seen the temperatures are much cooler than those observed. The lower left panel shows the model ground temperatures using the satellite derived moisture fields. As can be seen the ground temperatures are much closer to the satellite observed skin temperatures.

### ***Inferring grid scale heat capacity from satellite***

As mentioned above the surface heat capacity acts as a resistance to warming or cooling. While important, there are really no good methods for determining *a priori* the appropriate grid scale heat capacity. In the 2000 study period evening skin temperature tendencies as described above were used to infer a grid scale heat capacity. Figure 9 compares the satellite derived heat capacity with the benchmark or control heat capacity. On the broader scale it shows that smaller values of the slab heat capacity are associated with agriculture lands and prairies. Larger values are associated with more heavily vegetated areas. Moisture also plays a role. In the Texas area extremely dry conditions decreased the heat capacity values. Also, heavy rainfall in the upper mid-west increased the grid heat capacity.

Figure 10 shows the time evolution of the domain average value of surface moisture and heat capacity. Notice for both moisture and heat capacity that much of the adjustment occurs in the first few days as the number of grid points that are adjusted increases. Note also the relationship between moisture and heat capacity. While the satellite techniques for retrieving heat capacity and surface moisture are independent, the results indicate that the expected relationship of small heat capacities for drier conditions holds.

### ***Satellite skin temperature data as a model evaluation tool***

While the main thrust of this application activity was to provide satellite data to improve SIP modeling, we also used satellite skin temperatures as another technique to evaluate models. Standard National Weather Service stations are too widely separated to define temperature variations that can impact air quality on the mesoscale and the urban scale. However, satellite skin temperatures from GOES and MODIS provide a rich source of high resolution temperatures to evaluate models especially at small scales. In general, all models such as MM5 or WRF have a radiating temperature. Thus, the comparison of model radiating temperature and satellite skin temperature should be equivalent parameters (see caveat on this in the lessons learned section). Figure 11 shows an example of use of the spatial maps of model satellite temperature compared to model radiating ground temperature.

Figure 12 provides another depiction of model skill in that it compares paired in space and time scatter plots of the model radiating ground temperature and satellite skin temperature. Note that as the spatial resolution is increased that model performance substantially degrades. This is because the parameters that control surface temperatures such as moisture and heat capacity are highly uncertain. At large scales the inherent averaging of many land use types makes the average values of these parameters fairly good representation of the surface. However, as one moves to higher resolution then exact, spatially-paired values of these parameters are needed for

good temperature predictions. The satellite retrievals of these two key parameters are important for good model performance at high resolution. This is one of the most important benchmark comparisons under this study.

### ***Impact of satellite assimilation on 2 m air temperature***

While the comparison of model data to satellite data is a powerful evaluation tool, the traditional method of SIP model performance has been made by comparison with NWS standard observing network which nominally is a temperature measured 2 meters above the ground. Under the 2000 benchmarking period model predicted 2 meter air temperatures were compared to NWS observed temperatures. Figure 13 shows the comparison of model domain net bias as different levels of assimilation are included. Inclusion of all satellite information reduces the domain level bias. Figure 14 shows the spatial depiction of this mean bias and the root mean square error for the case with and without inclusion of the satellite data. By both measures the satellite data improves the simulation.

### ***Impact of satellite data on boundary layer heights***

The planetary boundary layer height or mixing height (in air quality terms) is a critical parameter that controls the entrainment of clean air and thus dilutes pollutant concentrations. The growth of the boundary layer is strongly dependent on the surface heat flux. As mentioned above the turbulent fluxes are critically dependent on the surface temperature which in turn is dependent on the insolation, moisture and heat capacity. These are the parameters targeted for improvement by the satellite information. Measures of boundary layer height are not a normal observable since standard rawinsondes occur too early or too late to capture maximum mixing heights during the day. During TEXAQS2000, special aircraft measurements were made which provided spatial variation on mixed layer height by the NOAA P3 aircraft. Figure 15 shows a comparison of planetary boundary layer heights for model simulations with and without the satellite data. It shows that the model simulation with the satellite data produced boundary layer heights in better agreement with observations from aircraft. Additionally, the model captured the spatial variation better in boundary layer heights.

### ***Impact of satellite photolysis fields on ozone production***

As mentioned above photolysis values are a first order parameter in photochemistry models. The techniques described above for using satellite cloud information to adjust photolysis rates were incorporated into the benchmark simulations for the 2000 period. Figure 16 shows the difference between ground level ozone for the cases with and without the satellite cloud adjustments. Baseline runs under this activity showed that incorporating the satellite data improved the photolysis rates and changed ozone levels in the model by up to 70 ppb at some points in the domain. The top panel shows substantial spatial differences between the cases with and without satellite adjustments. The lower panel shows that the satellite data improves ozone prediction compared to time series of observations.

When ozone levels exceed air quality standards, states must adopt emission reductions to lower levels based on models. It may cost industry and the public billions to reduce ozone levels by 20-30 ppb. Thus, the differences in modeled ozone levels (70 ppb) due to the satellite photolysis technique are huge relative to reductions needed. Both EPA and Texas recognized that

improving the photolysis rates were critical to confidence in the models. For example if photolysis rates are too low then emission reductions will be less effective causing over-control of industry at significant costs. Alternatively, photolysis rates which are too high may over-estimate the impact of emission reductions leading to a failure of regulations to meet air quality standards. Confidence in models is critical for industry to accept the regulations without challenge.

### ***Impact of MODIS emissivity in the surface energy budget***

While the techniques described above had been tested in a research setting, the use of MODIS emissivity was new under this activity. Tests of the MODIS emissivity products were made both in the model and in the GOES LST retrievals (see Suggs et al. 2000). Based on the results in Suggs et al. 2000 there was some uncertainty in the use of the spectral emissivities in the broad band application in the model. Nevertheless, MODIS emissivities based on two channels were tested in the model. There were no significant differences found. There was also concern that there were problems with the MODIS emissivities for use in LST retrievals. Suggs et al. 2000 showed that use of MODIS level 3 emissivities in the GOES retrievals actually caused more differences between MODIS LST retrievals and GOES and GOES retrievals. This was unexpected. There were concerns about whether differences in MODIS channel emissivities were real. Because of these concerns and the fact that use of the MODIS emissivities might degrade GOES LST retrievals and uncertainty in the use of these products in the surface energy budget, this activity was terminated. It may be useful for future study.

### **Insolation impact during the 2006 modeling period**

In addition to the 2000 period the satellite techniques were tested for a longer period July 1-September 30, 2006. This was also the first test of the albedo and insolation technique in the WRF model. We simulated a case of Aug. 6-10, 2006 using the WRF model with and without GOES data assimilation. Figure 17 shows the shortwave radiation plots with and without the GOES data at 19GMT on Aug. 9, 2006. Figure 17 (lower panel) shows the differences of the shortwave radiation with and without GOES data assimilation at the same time. Even though the color schemes are slightly different, it is noticeable that the biggest differences of the surface shortwave radiation flux occurred at the area surrounding the mouth of Mississippi River and Gulf of Mexico and where Indiana, Ohio, and Kentucky meet. Note the differences are large and can make large differences in surface temperature. In comparison to NWS analyses the shortwave radiation reaching the ground in the WRF simulation with GOES data assimilation shows much better agreement with observations. Note that there are some discontinuities in the solar insolation field due to missing data in GOES observations in the northern portion of the domain. To overcome this we can cut the missing data region while running MCIP so CMAQ simulations are not affected.

## **VIII. Transition of Products to the User Community**

SIP modeling is carried out by state and local governments some times in collaboration with the U.S. EPA and private consultants. Because of the results from the benchmark studies and positive feedback and use of the satellite data by Texas and consultants as part of this project we

are providing a system that serves the satellite data and tools to the broad U.S. air quality community. This has been done in association with Marshall Space Flight Center (MSFC) Earth Observing System (EOS) data center (the Global Hydrology Resource Center (GHRC, <http://ghrc.msfc.nasa.gov>). A site has been established to provide background information, data and tools to use the data within the CMAQ system.

This site serves as a gateway for obtaining satellite data to be utilized in air quality modeling practices. It specifically targets the needs of regulatory community by providing tools and documentation necessary for incorporating satellite data into EPA's WRF/MM5/CMAQ air quality modeling system. CMAQ is routinely used in the SIP modeling practices in which emission-reduction strategies are defined to reduce air pollution concentrations to levels that meet the NAAQS.

The links from this page provide access to data products from GOES and from MODIS. GOES products comprise short wave radiation incident at the surface (insolation), surface albedo, skin temperature, cloud top albedo and pressure. Surface insolation and skin temperature are crucial in the boundary layer development (McNider et al. 1994, 1995, 2005), while clouds affect many aspects of transport and transformation of pollutants in the atmosphere including significantly altering the solar radiation in the wavelengths affecting the photolysis rates and thereby impacting the photochemistry considerably. The users of this site can also download the necessary tools and detailed documentation for the utilization of these data in CMAQ modeling system.

One of the major achievements under this activity was that EPA has included the satellite albedo, solar insolation and photolysis adjustments in its formal release of the CMAQ system. The technique was incorporated into EPA's CMAQ System and was made part of EPA's official release of the CMAQ version 4.7. Additionally, the State of Texas incorporated the technique into their CAMX SIP model.

## **IX. Lessons Learned and Recommendations**

While we believe that the benchmarking was successful and showed the benefit of the satellite techniques, as part of this process we have found some things which may impact the utility and broad applicability of techniques. These are outlined below.

### ***Over-drying of the atmosphere using the satellite adjustment of surface moisture***

While the benchmarking studies showed that the adjustment of surface moisture and heat capacity improved the temperature performance of the MM5 both in comparison to satellite skin temperatures and NWS air temperatures, it was determined that the adjustment over-dried the atmosphere. Figure 18 shows comparisons of model and NWS specific humidity with and without satellite adjustments. It shows that the initial model control run was too moist with respect to observed dew points. The satellite adjustment did dry out the model and this was the source of the improvement in temperature performance. However, further study showed that the satellite technique over-dried the surface making the model specific humidity lower than observed. The goal of the McNider et al. (1994) assimilation technique was to provide more realistic land surface forcing by adjusting the moisture availability within the latent heat flux

term of the surface energy budget. Thus, the technique should theoretically improve the moisture specification not degrade it. In fact the original testing of the model in McNider et al. (1994) showed this to be the case. A concerted effort was made to determine what aspect or assumptions in the McNider et al. (1994) technique might be leading to this discrepancy. It has been determined that a discrepancy exists when implementing the technique within the framework of the MM5. The root of this problem lies within a physical inconsistency in the formulation of surface temperature in the MM5 for which the ground temperature is used for all processes that require a near-surface temperature both for fluxes and radiation. The ground temperature was used as the radiating temperature. Thus, initially it was felt that this was the appropriate temperature to be used in comparison to the satellite radiating skin temperature. However, it was determined that the finite heat capacity of the slab reduced its dynamic range in response to forcing. A correction was made to deduce a true skin temperature. The original McNider et al. (1994) formulation used a skin temperature but in the transition to MM5 used the ground temperature. However, a second issue was found in that this true skin temperature cannot be used in the flux calculation rather an aerodynamic temperature is needed. The original McNider et al. (1994) formulation did calculate an aerodynamic temperature. The importance of the consistent use of aerodynamic temperature is well studied within the boundary layer community but has not always been adhered to in the mesoscale model community as evidenced by developments within MM5. The inconsistency typically only surfaces when an investigator attempts to use measurements of skin temperature or recover that temperature from a diagnostic surface energy budget (Sun and Mahrt 1995; Beljaars and Holtlag 1991).

An investigation took place to make a first attempt to recover a model skin temperature within the MM5 framework for direct comparison with the information provided by the satellite retrievals and use of a correct aerodynamic temperature. This study and its testing are reported in Mackaro (2008). However, this solution was not timely enough to be retested in the benchmark setting. Tests in Mackaro (2008) and Mackaro et al. (2008) using a true skin temperature and aerodynamic temperature show that the new formulation can improve both the temperature and dew point performance.

### ***Issues with GOES sensor calibration***

As part of this activity, a system that could deliver the tools and satellite data was developed. The satellite data is processed in real-time each day as part of the NASA Short-term Prediction Research and Transition Center (SPoRT) activity and the MSFC GHRC. This system appears to work well in building a long-term archive for use by the air quality community. However, as the project progressed we found that degradation in the on-board visible sensor was causing retrieved products such as surface albedo to also become degraded. While we were able make adjustments in the data for the 2000 benchmark period by reprocessing the data, it means that data for other periods remains uncorrected especially data under the new GOES 12. We are exploring options for correcting the data which will not require full reprocessing. This may be in the form of an additional utility that will operate in conjunction with regridding software to make the sensor adjustments. However, resources for developing this tool have not been identified.

## X. References

- Allen, C. W., 1963: *Astrophysical Quantities*, 291 pp., Athlone Press, London.
- Anthes, R.A. and T.T. Warner, 1978: Development of hydrodynamic models suitable for air-pollution and other mesometeorological studies. *Mon. Wea. Rev.*, **106**, 1045-1078.
- Arola, A., S. Kalliskota, P. N. den Outer, K. Edvardsen, G. Hansen, T. Koskela, T. J. Martin, J. Matthijsen, R. Meerkoetter, P. Peeters, G. Seckmeyer, P. C. Simon, H. Slaper, P. Taalas and J. Verdebout, 2002: Assessment of four methods to estimate surface UV radiation using satellite data, by comparison with ground measurements from four stations in Europe, *J. Geophys. Res.*, **107**(D16), 4310, doi:10.1029/2001JD000462.
- Beljaars, A. C. M. and A. A. M. Holtslag. 1991. Flux Parameterization over Land Surfaces for Atmospheric Models. *Journal of Applied Meteorology* 30:327-341.
- Blackadar, A. K., 1979: High resolution models of the planetary boundary layer. *Adv. Environ. Sci. Eng.*, **1**, 50- 85.
- Brewer J., P. Dolwick, and R. Gilliam. 2007. Regional and Local Scale Evaluation of MM5 Meteorological Fields for Various Air Quality Modeling Applications, Presented at the 87th Annual American Meteorological Society Annual Meeting, San Antonio, TX, January 15-18, 2007.
- Carlson, T. N., 1986: Regional scale estimates of surface moisture availability and thermal inertia using remote thermal measurements. *Remote Sensing Rev.*, **1**, 197-246.
- Chang, J. S., R. A. Brost, I. S. A. Isaksen, S. Madronich, P. Middleton, W. R. Stockwell and C. J. Walcek, 1987: A three-dimensional Eulerian acid deposition model: Physical concepts and formulation, *J. Geophys. Res.*, **92**(D12), 14,681–14,700.
- Collins, D. R., H. H. Jonsson, H. Liao, R. C. Flagan, J. H. Seinfeld, K. J. Noone and S. V. Hering, 2000: Airborne analysis of the Los Angeles aerosol, *Atmos. Environ.*, **34**(24), 4155–4173.
- Coulson, K. L., 1959: Characteristics of the radiation emerging from the top of a Rayleigh atmosphere, 1 and 2, *Planet. Space Sci.*, **1**, 256– 284.
- Deardorff, J. W., 1972: Theoretical expression for the countergradient vertical heat flux. *J. Geophys. Res.*, **77**, 5900-5904.
- Diak, G. R., C. Gautier, 1983: Improvements to a simple physical model for estimating insolation from GOES data. *J. Appl. Meteor.*, **22**, 505-508.
- Diak, G. and M. Whipple, 1995: Note on estimating surface sensible heat fluxes using surface temperatures measured from geostationary satellite. *J. Geophys. Res.*, **100**, 25453-25461
- Dickerson, R. R., S. Kondragunta, G. Stenchikov, K. L. Civerolo, B. G. Doddridge and B. N. Holben, 1997: The impact of aerosols on solar ultraviolet radiation and photochemical smog, *Science*, **278**, 827– 830.
- Dickinson, R.E., 1984: Modeling evapotranspiration for three global climate models, in *Climate Process and Climate Sensitivity. Geophys. Monogr. Ser.* **29**, edited by J. Harrison and T. Takahashi, pp 58-72, AGU, Washington D.C.

Dudhia, J. and J.F. Bresch, 2002: A global version of the PSU-NCAR Mesoscale Model. *Mon. Wea. Rev.*, **130**, 2989-3007.

EPA, 1999: Science algorithms of the EPA Models-3 Community Multiscale Air Quality (CMAQ) modeling system, EPA-600/R-99/030, Washington, DC.

Fritz, S., and J. S. Winston, 1962: Synoptic use of radiation measurements from satellite TIROS-II, *Mon. Weather Rev.*, **90**, 1–9.

Gautier, C., G. R. Diak, and S. Mass, 1980: A simple physical model for estimating incident solar radiation at the surface from GOES satellite data. *J. Appl. Meteor.*, **19**, 1005-1012.

Gillies, R.R. and T.N. Carlson, 1995. Thermal remote sensing of surface soil water content with partial vegetation cover for incorporation into climate models. *J. Appl. Meteor.*, **34**, 745-756.

Grell, G. A., J. Dudhia and D. R. Stauffer, 1994: A description of the Fifth-Generation Penn State/NCAR Mesoscale Model (MM5), NCAR Tech. Note, NCAR/TN-398+STR, 138 pp., Natl. Cent. for Atmos. Res., Boulder, CO.

Haines, S. L., R. J. Suggs, and G. J. Jedlovec, 2004: The Geostationary Operational Environmental Satellite (GOES) product generation system, NASA Tech. Memo., NASA TM-2004-213286. (Available at <http://hdl.handle.net/2060/20050019524>).

Jacobson, M. Z., 1998: Studying the effects of aerosols on vertical photolysis rate coefficient and temperature profiles over an urban airshed, *J. Geophys. Res.*, **103**(D9), 10,593–10,604.

Jedlovec, G. J., J. A. Lerner, and R. J. Atkinson, 2000: A satellite-derived upper-tropospheric water vapor transport index for climate studies, *J. Appl. Meteorol.*, **39**, 15– 41.

Jiang, L. and Islam, S., 1999: A methodology for estimation of evapotranspiration over large areas using remote sensing information. *Geophysical Research Letters* **26**(17), 2773-2776.

Kemball-Cook, S., Y. Jia, C. Emery, R. Morris, Z. Wang, and G. Tonnesen. 2005. Annual 2002 MM5 Meteorological Modeling to Support Regional Haze Modeling of the Western United States, Prepared for The Western Regional Air Partnership (WRAP), 1515 Cleveland Place, Suite 200 Denver, CO 80202, March 2005.

Lacis, A. A., and J. E. Hansen, 1974: A parameterization for absorption of solar radiation in the Earth's atmosphere, *J. Atmos. Sci.*, **31**, 118–133.

Lapenta, W. M., R. Suggs, G. J. Jedlovec, and R. T. McNider, 1999: Impact of assimilating GOES-derived land surface variables into the PSU/NCAR MM5. *Preprints, Workshop on Land-Surface Modeling and Applications to Mesoscale Models*, NCAR, Boulder CO, 65-68.

Liao, H., Y. L. Yung and J. H. Seinfeld, 1999: Effects of aerosols on tropospheric photolysis rates in clear and cloudy atmospheres, *J. Geophys. Res.*, **104**(D19), 23,697–23,708.

Mackaro, S., 2008: The importance of physically consistent temperature representation in land surface satellite assimilation, Ph.D. Dissertation, Atmospheric Science Department, University of Alabama in Huntsville, 157pp.

Mackaro, S., M., R. T. McNider, A. Pour-Biazar, A Physically Consistent Method for the Assimilation of Land Surface Temperature Tendencies, in *Proceedings of American Meteorological Society 88<sup>th</sup> Annual Meeting, 12th Conference on Integrated Observing and*

*Assimilation Systems-Assimilation of Ocean and Land Surface Observations into Models-I (12IOAS-AOLS)*, New Orleans, LA, January 20-24, 2008.

McCumber, M. C. and R. A. Pielke, 1981: Simulations of the effects of surface fluxes of heat and moisture in a mesoscale numerical model. 1: Soil layer. *J. Geophys. Res.*, **86**, 9929–9938.

McNider, R.T., A.J. Song, D.M. Casey, P.J. Wetzel, W.L. Crosson, and R.M. Rabin, 1994: Toward a dynamic-thermodynamic assimilation of satellite surface temperature in numerical atmospheric models. *Mon. Wea. Rev.*, **122**, 2784-2803.

McNider, R. T., J. A. Song, and S. Q. Kidder, 1995: Assimilation of GOES-derived solar insolation into a mesoscale model for studies of cloud shading effects. *Int. J. Remote Sens.*, **16**, 2207-2231.

McNider, R. T., W. B. Norris, D. M. Casey, J. E. Pleim, S. J. Roselle and W. M. Lapenta, 1998: Assimilation of satellite data in regional scale models, in *Air Pollution Modeling and Its Application XII*, NATO Challenges of Modern Soc., vol. 22, edited by S. E. Gryning and N. Chaumerliac, pp. 25–35, Springer, New York.

Paltridge, G. W., 1973: Direct measurement of water vapor absorption of solar radiation in the free atmosphere, *J. Atmos. Sci.*, **30**, 156–160.

Pielke, R. A., G. A. Dalu, J. S. Snook, T. J. Lee, and T. G. F. Kittel, 1991: Nonlinear influence of mesoscale land use on weather and climate. *J. Climate*, **4**, 1053–1069.

Price, J. C., 1982: On the use of satellite data to infer surface fluxes at meteorological scales. *J. Appl. Meteor.*, **21**, 1111-1122.

Pour-Biazar, A., R. T. McNider, S. J. Roselle, R. Suggs, G. Jedlovec, D. W. Byun, S. Kim, C. J. Lin, T. C. Ho, S. Haines, B. Dornblaser and R. Cameron, 2007: Correcting photolysis rates on the basis of satellite observed clouds. *J. Geophys. Res.*, **112**, D10302, doi:10.1029/2006JD007422.

Sellers, P.J., Y. Mintz, Y. Sud, and A. Dalcher, 1986: A simple biosphere model (SiB) for use with general circulation models, *J. Atmos. Sci.*, **43**, 505-531.

Smirnova, T. G., J. M. Brown, S. G. Benjamin, 1997: Performance of Different Soil Model Configurations in Simulating Ground Surface Temperature and Surface Fluxes. *Mon. Wea. Rev.*, **125**, 1870–1884.

Suggs, R.J., S. Haines, G.J. Jedlovec, W.M. Lapenta, and D. Moss, 2000: Land Surface Temperature Retrievals from GOES-8 Using Emissivities Retrieved from MODIS, [http://ams.confex.com/ams/annual2003/techprogram/program\\_144.htm](http://ams.confex.com/ams/annual2003/techprogram/program_144.htm), 83rd AMS Annual Meeting, Long Beach, CA, February 13, 2003.

Sun, J. and L. Mahrt, 1995: Determination of Surface Fluxes from the Surface Radiative Temperature. *Journal of the Atmospheric Sciences*, **52**, 1096-1106.

Wetzel, P. J., 1978: A detailed parameterization of the atmospheric boundary layer. Ph.D. dissertation, Colorado State University, 165 pp.

Wetzel, P. J., 1984: Determining soil moisture from geosynchronous satellite infrared data: A feasibility study. *J. Climate Appl. Meteor.*, **23**, 375-391.

Zhang, D., and R. A. Anthes, 1982: A high-resolution model of the planetary boundary layer—Sensitivity tests and comparisons with SESAME-79 data. *J. Appl. Meteor.*, **21**, 1594-1609.

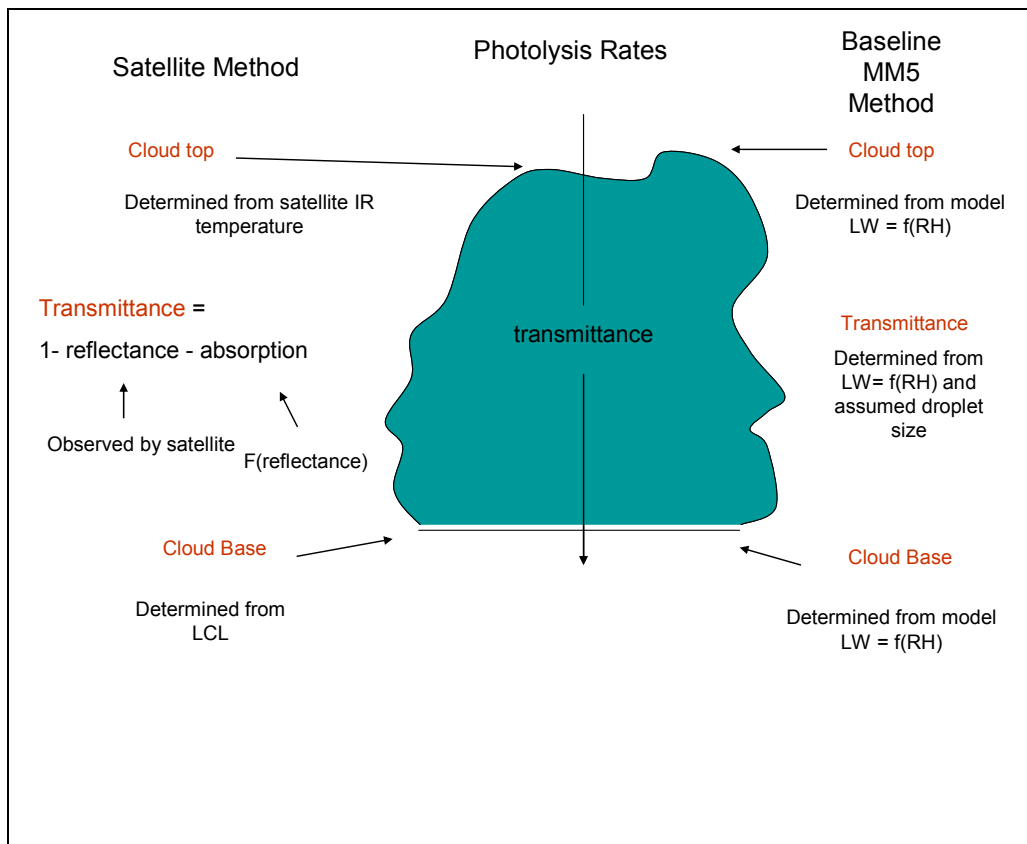


Figure 1. Example schematic of how satellite data are used to replace cloud model variables needed to make cloud adjustments to photolysis rates in the CMAQ system.

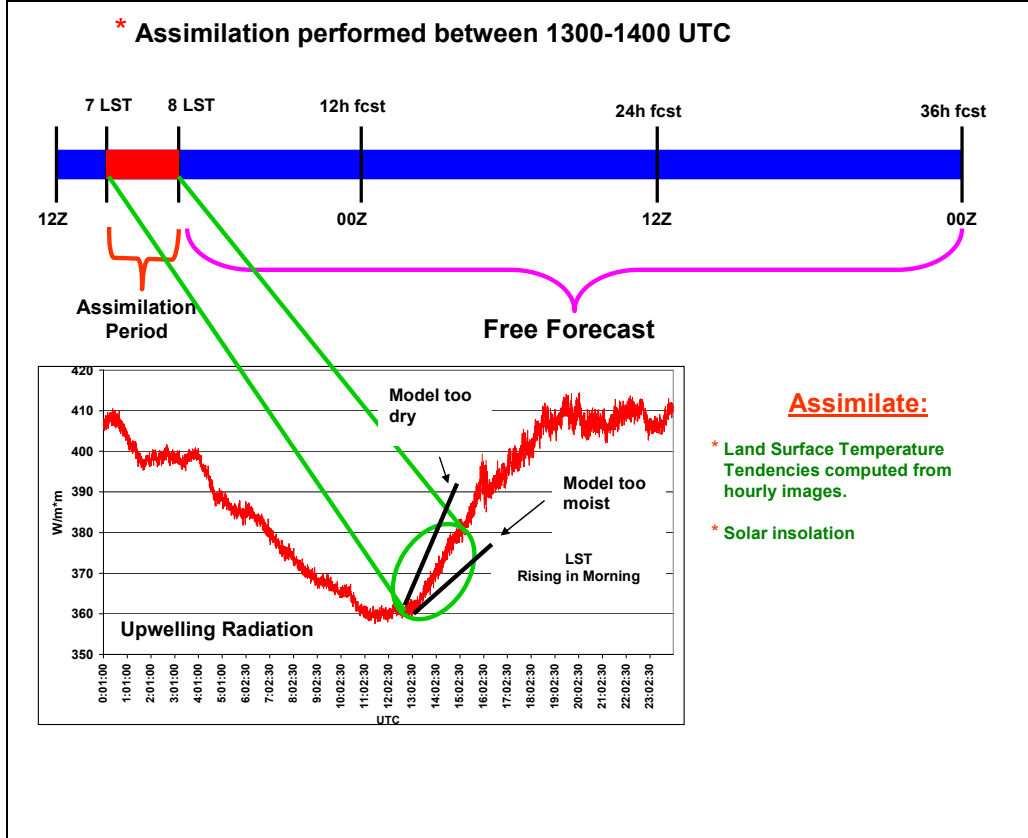


Figure 2. Example schematic of how satellite skin temperature tendencies are used to adjust soil moisture. Based on the difference in tendencies between the model and satellite during the morning period the surface moisture is adjusted using equation (6). Note that satellite temperatures are not directly assimilated but are used to adjust moisture.

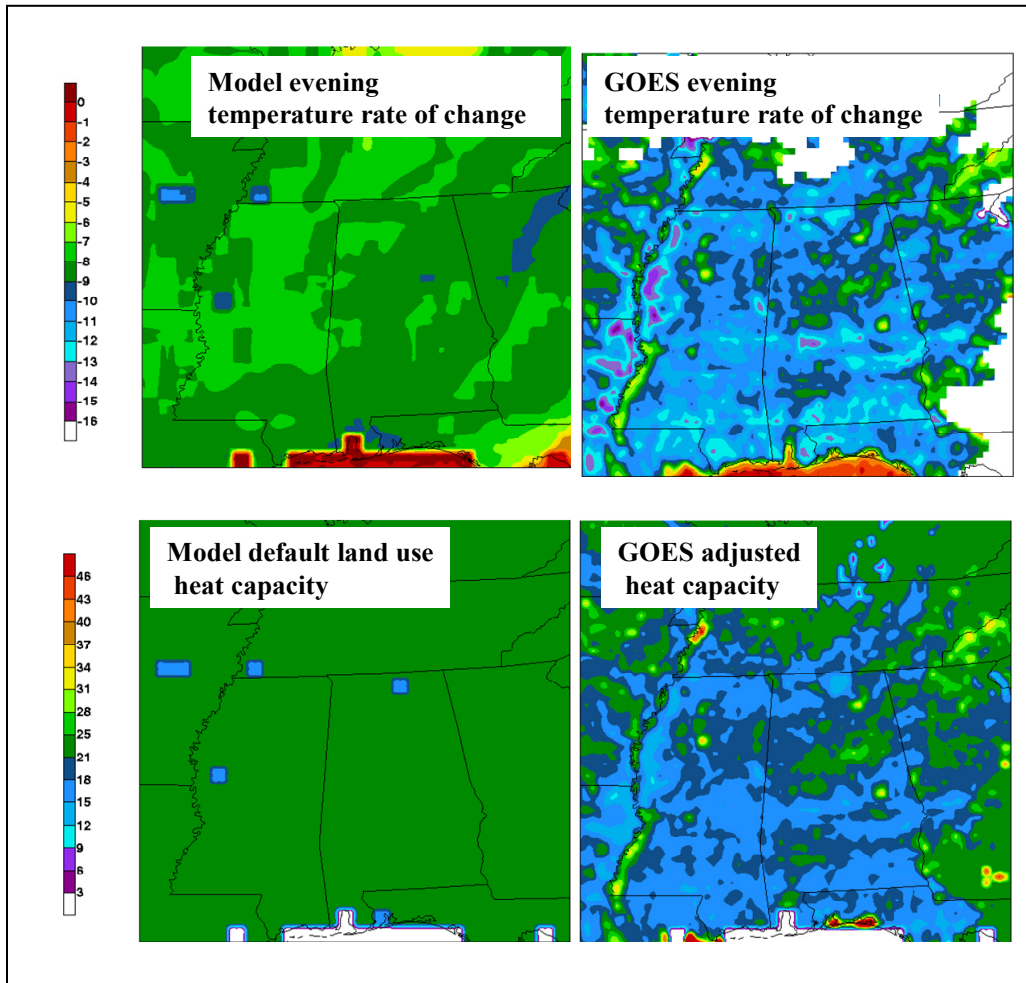


Figure 3. Upper left: evening skin temperature tendency from the model using MM5 standard heat capacity values. Upper right: evening skin temperature tendencies observed by GOES. Lower left: default heat capacity values in the land use table used in MM5 for the 25 class USGS land use scheme. Lower right: derived heat capacity using equation (7) [from McNider *et al.* 2005].

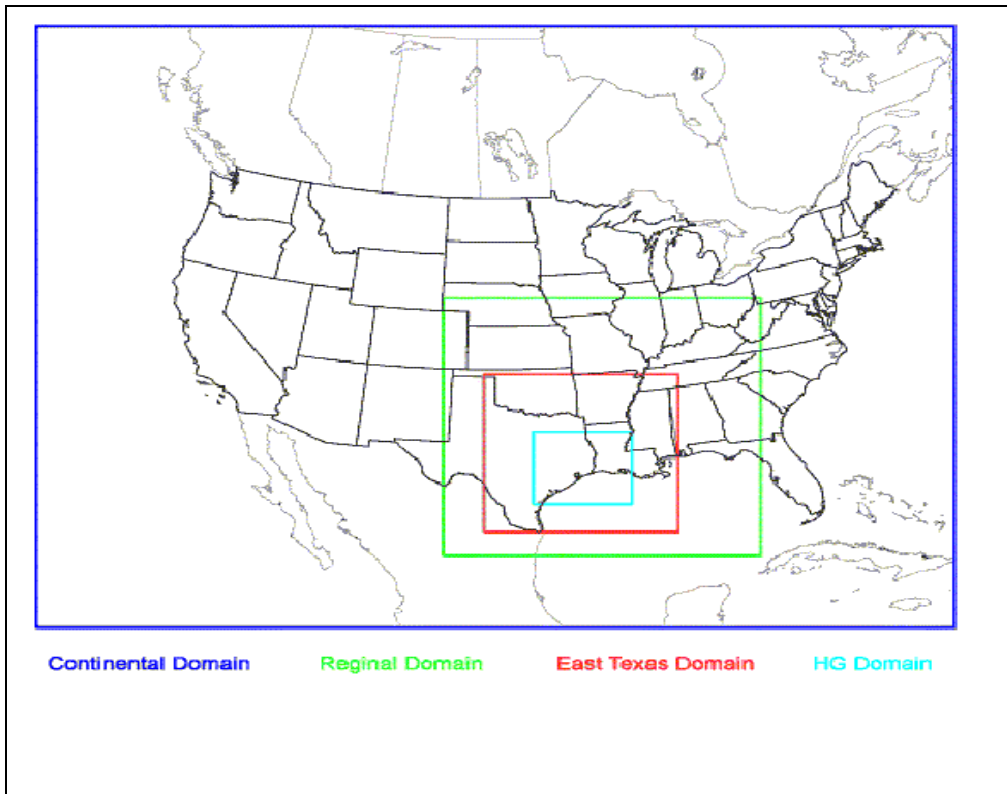


Figure 4. Modeling domains for TexAQS2000 modeling episode.

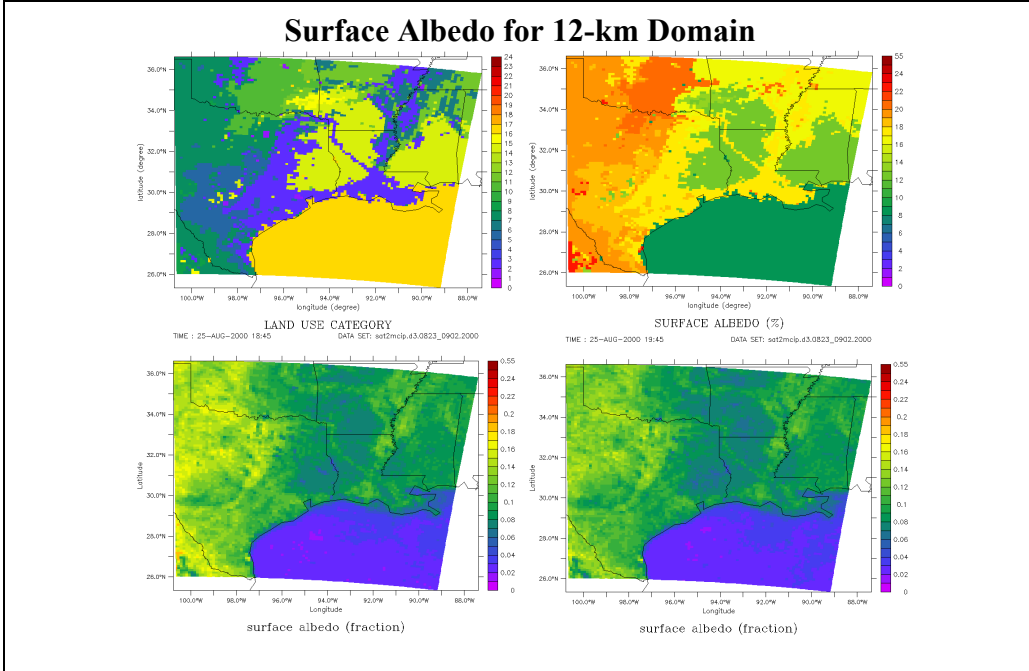


Figure 5. Example of use of satellite albedo during the 2000 benchmark period. Upper left: land use classifications which are normally used to specify land surface parameters such as albedo. Upper right: albedo based on the land use classes. Lower panels: 30 day satellite derived albedo at two different times. While land use class specification of albedo captures the broad aspects of albedo they cannot capture the dynamic changes due to plant phenology.

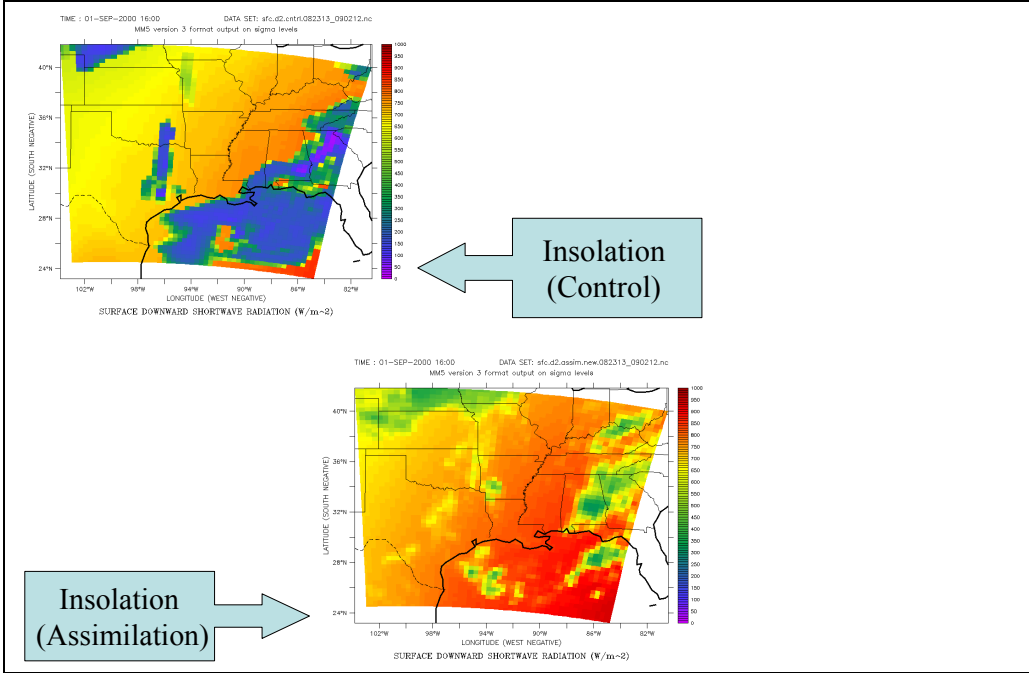


Figure 6. Comparison of surface insolation where model clouds impact insolation values (upper left -control) with satellite derived insolation values (lower right – assimilation).

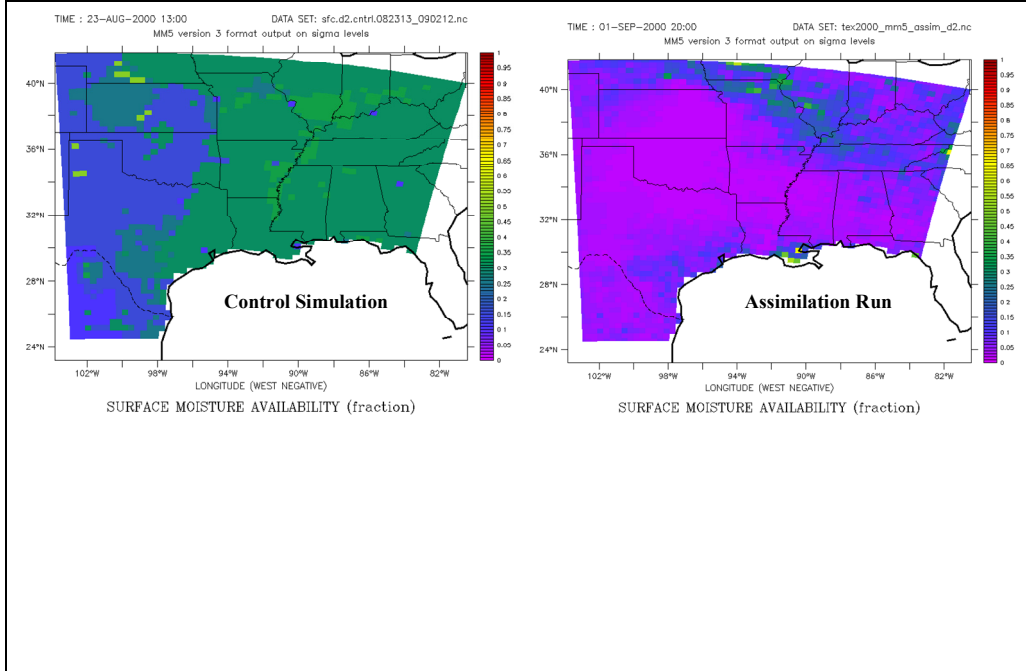


Figure 7. Left: climatological moisture values from the land use classifications used in the baseline run. Right: retrieved surface moisture using the satellite skin tendencies to adjust the baseline moisture.

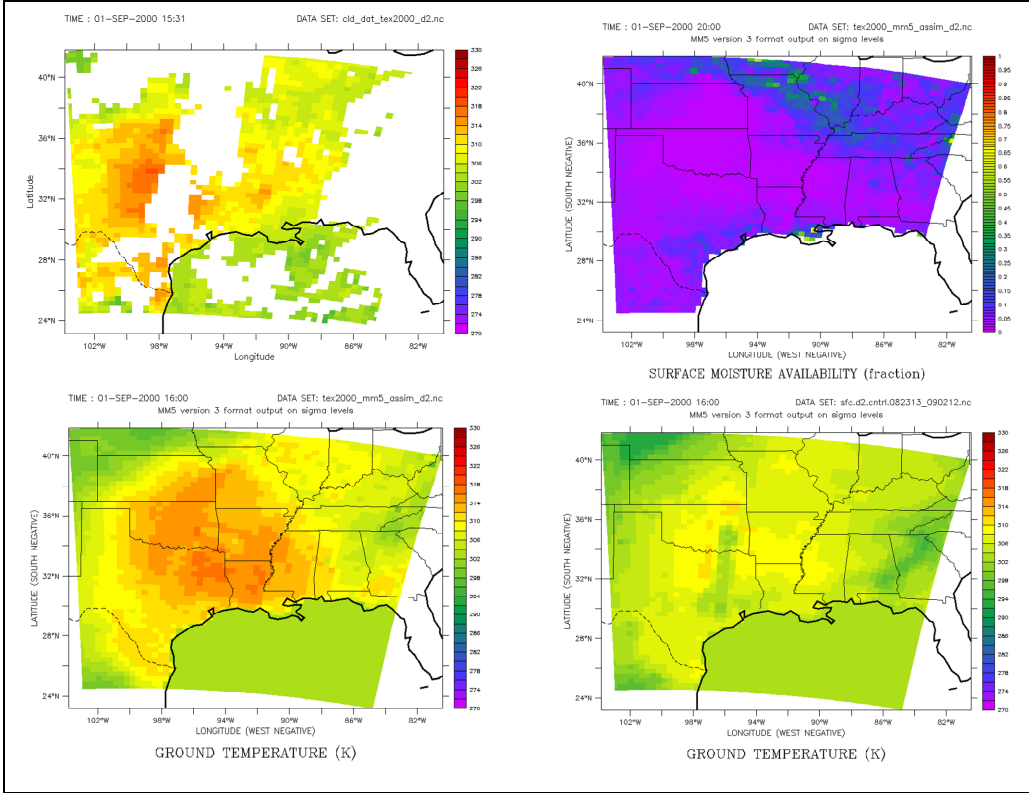


Figure 8. Illustration of the impact of surface moisture assimilation on skin temperature differences between the baseline case and the case with satellite assimilation. Upper left: satellite observed surface skin temperature. Upper right: retrieved surface moisture using equation (6). Bottom left: predicted ground surface temperatures using the satellite retrieved surface moisture. Bottom right: default benchmark temperatures without satellite data.

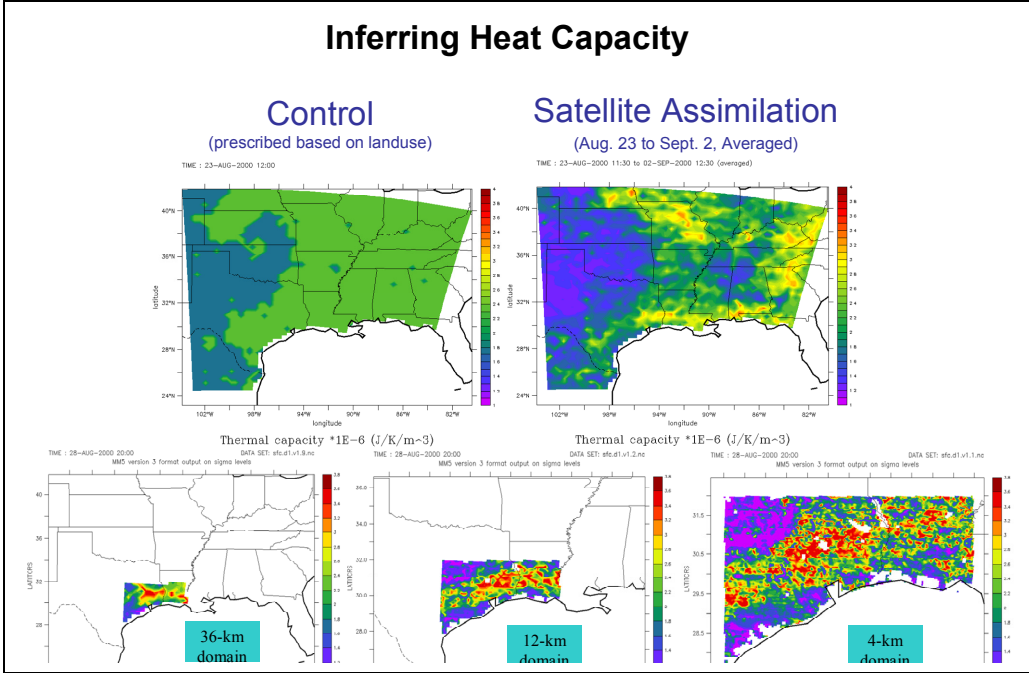


Figure 9. Comparison of grid scale heat capacity values using the MM5 baseline method of land use classes with the satellite derived values using equation (7). Upper left: values from the land use classes. Upper right: heat capacity values as retrieved from the satellite technique.

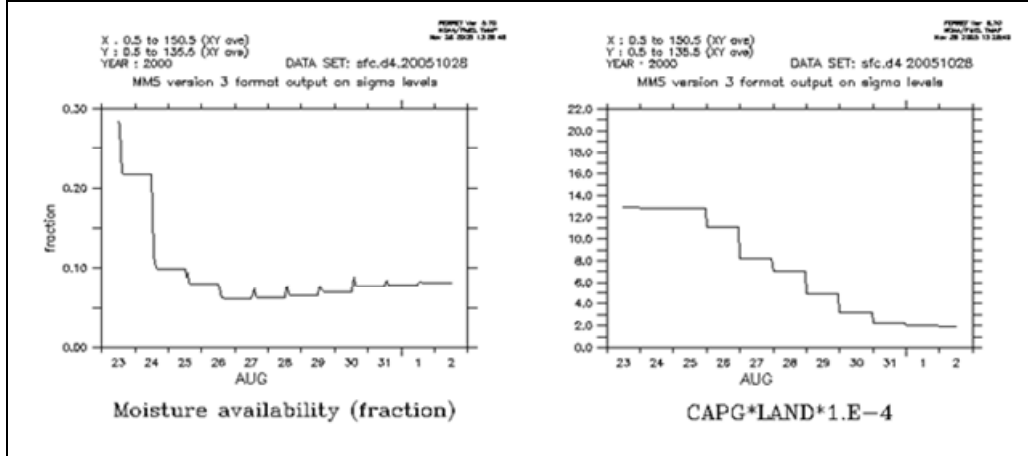


Figure 10. The evolution of surface moisture and grid scale heat capacity during the 2000 benchmark period. Left: time evolution of the satellite retrieved surface moisture average over the whole 12km domain. Right: corresponding change in grid scale heat capacity.

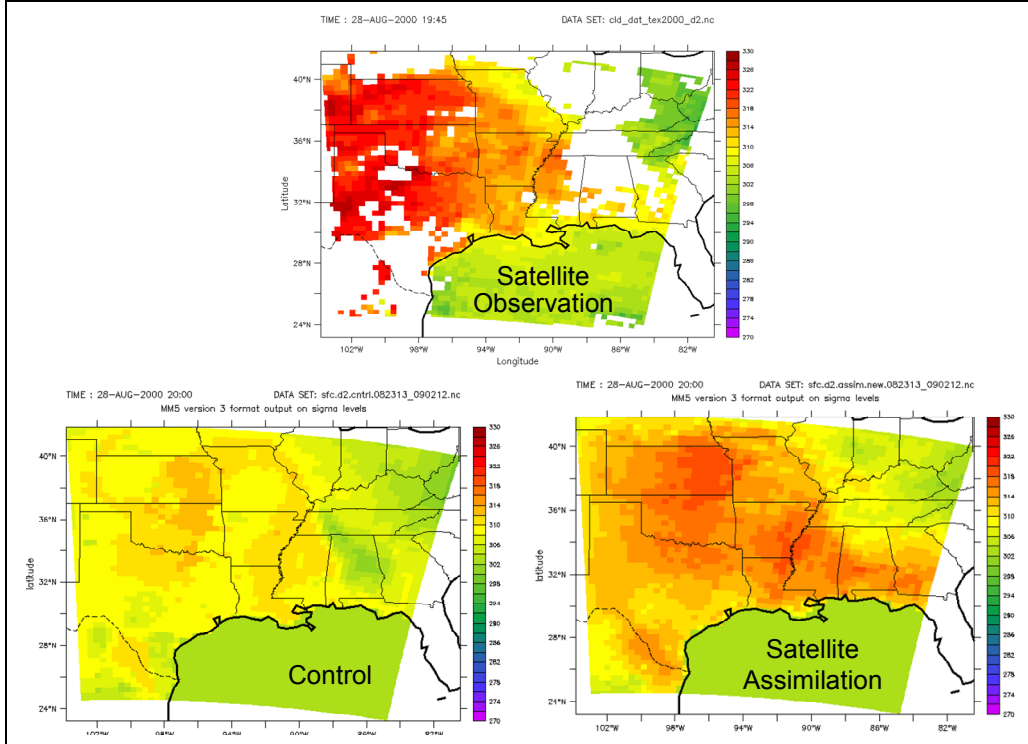


Figure 11. Comparison of satellite skin temperatures and corresponding ground radiating temperatures in MM5 for a day during the 2000 experiment. Upper panel: 16:00 GOES skin temperature. Lower panels: ground radiating temperature for both the control benchmark run and the case where satellite insolation, satellite albedo, satellite derived surface moisture and satellite derived heat capacity were used in the model run.

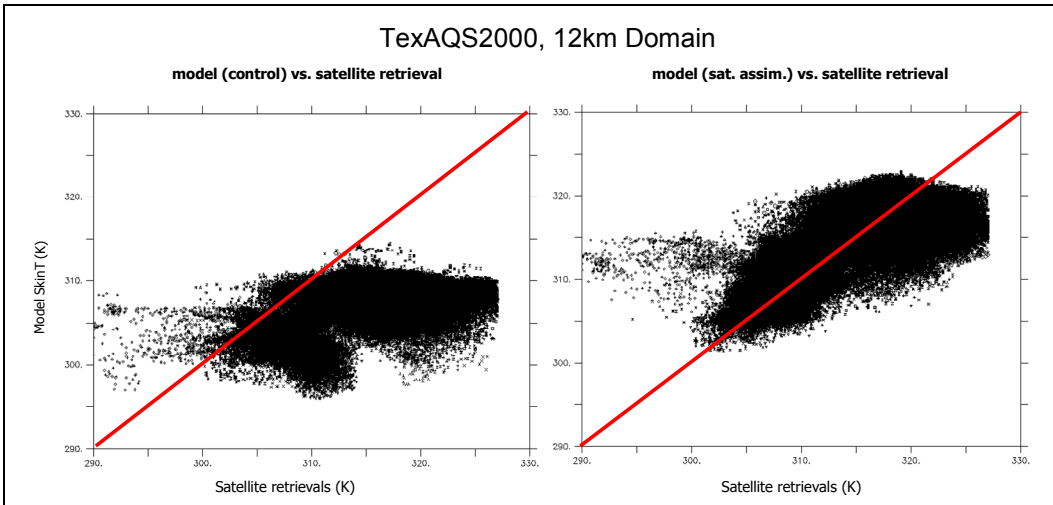
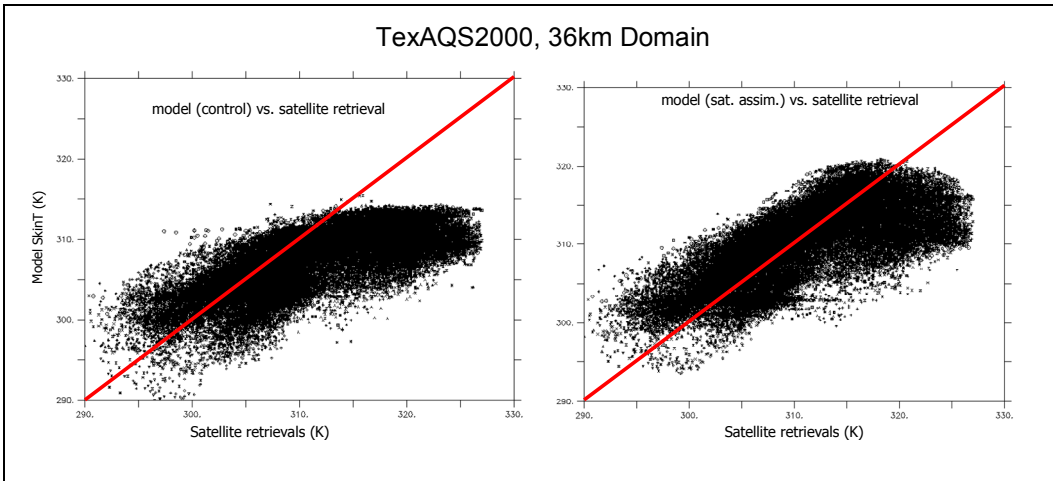
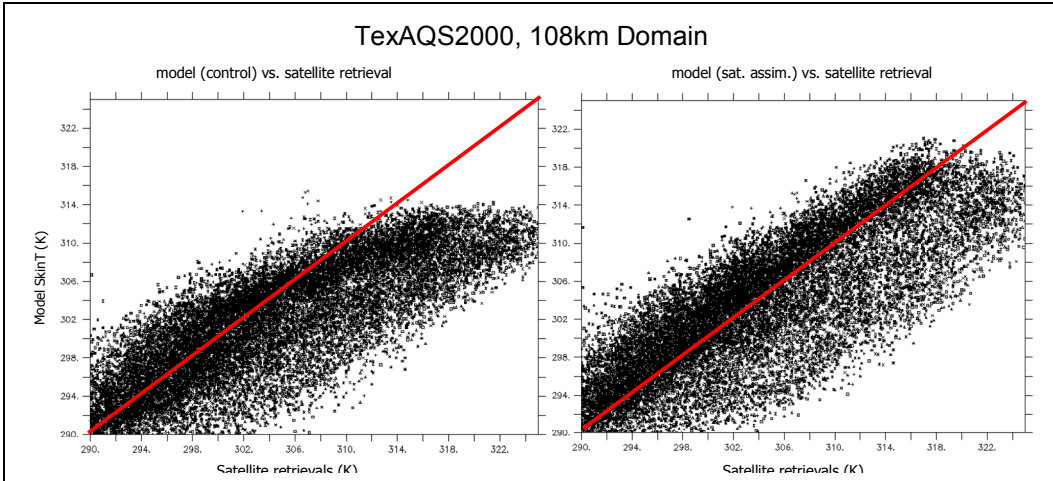


Figure 12. Example of the use of satellite skin temperatures compared to model radiating ground temperatures as a model evaluation tool. Note that model performance without satellite assimilation degrades as finer resolution is employed.

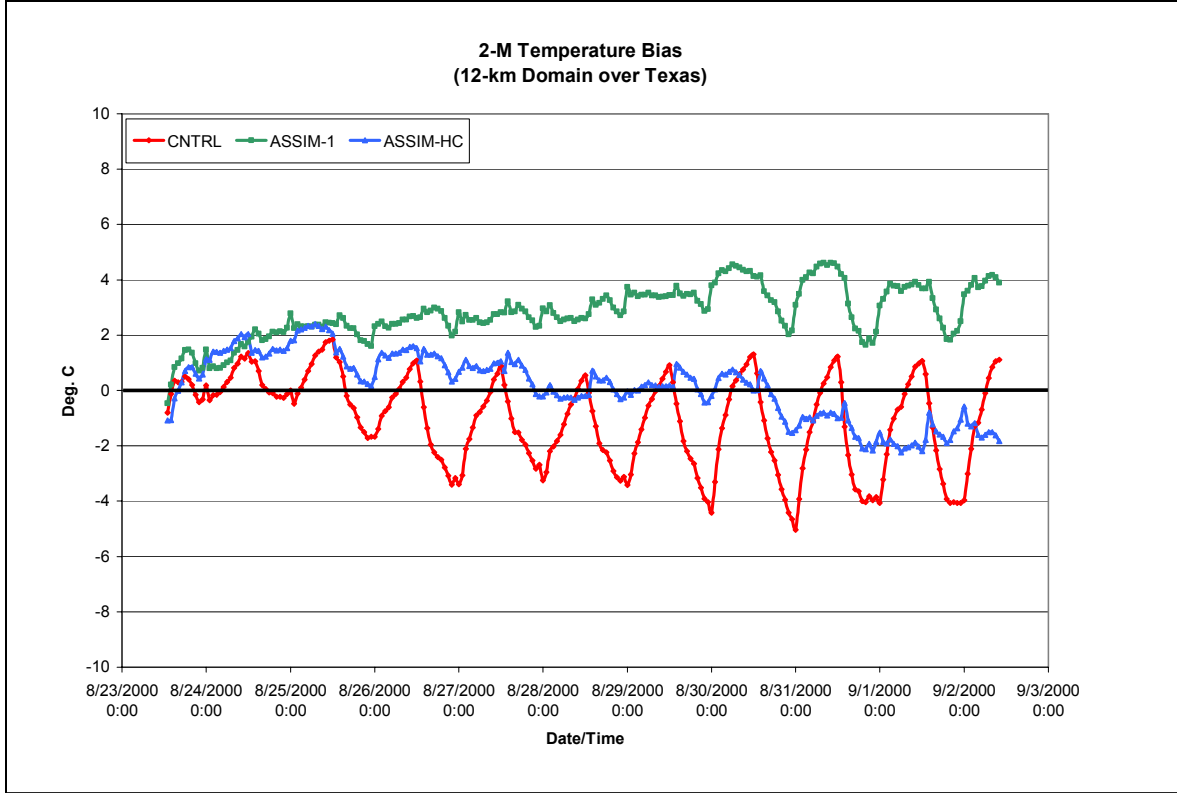


Figure 13. Depiction of model bias as satellite data are added. The red line shows the control experiment without satellite data. Note in general daytime under-prediction of temperatures and nighttime over-prediction. Blue line gives bias after inclusion of satellite insolation, albedo and moisture adjustment is made. Increases in temperature change bias to positive (over-prediction).. Inclusion of heat capacity reduces the net bias.

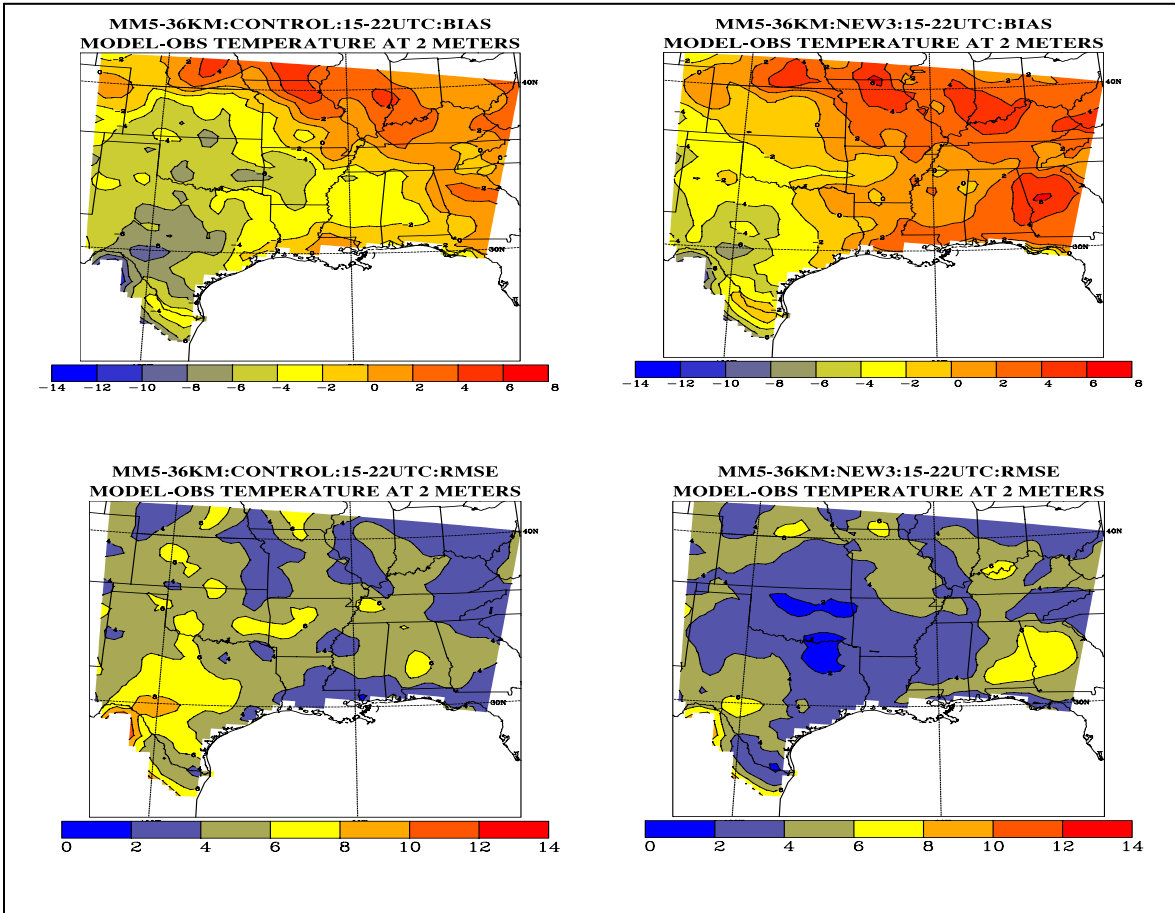


Figure 14. Depiction of spatial model performance compared to NWA 2m air temperatures with and without satellite data. Top: mean bias with satellite (right) and without satellite data (left). Lower panel: same for root mean square error.



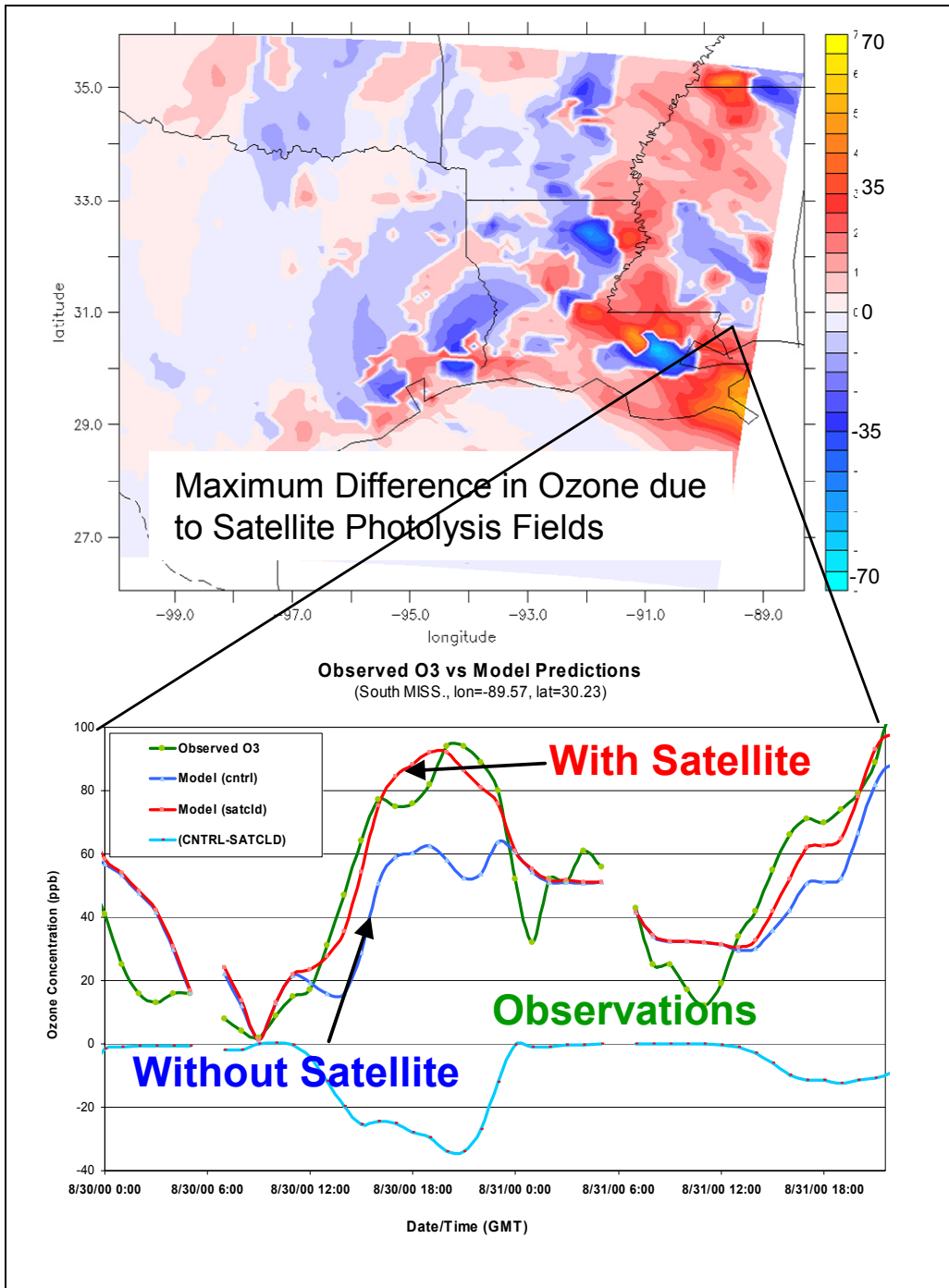


Figure 16. Top: differences in ozone between two CMAQ runs with and without use of satellite derived photolysis fields. Note the maximum differences exceed 50 ppb. Bottom: time series of ozone prediction from the model vs. observations at an EPA monitoring site in South Mississippi.

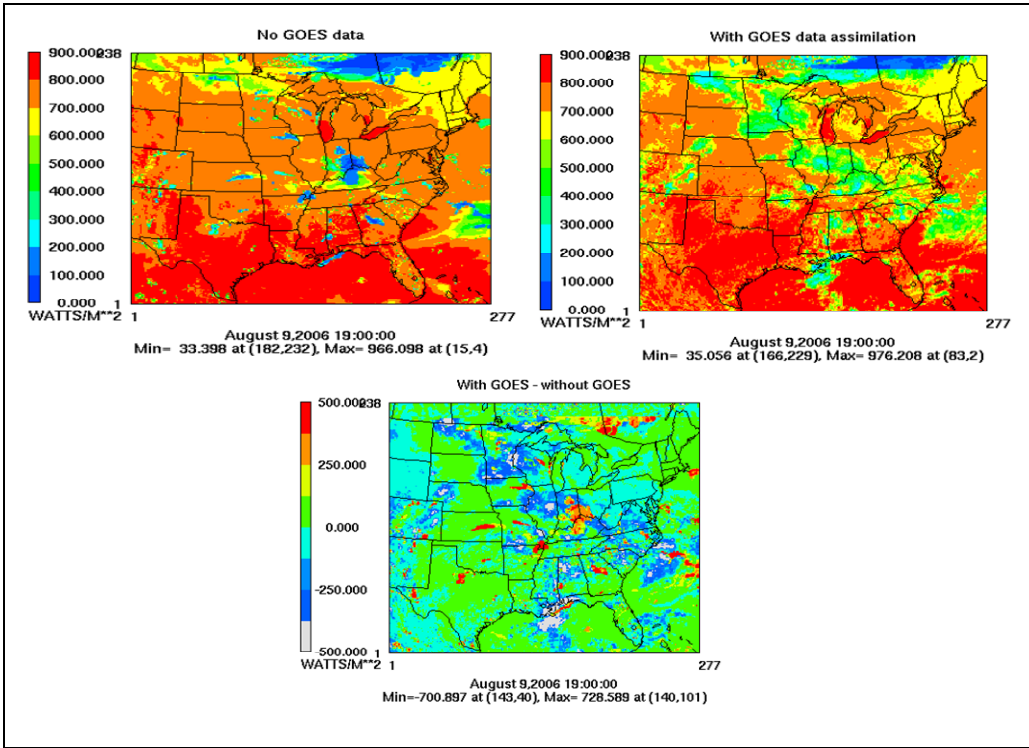


Figure 17. Comparisons of surface insolation with and without satellite data in the WRF model. Upper left: insolation values using WRF generated clouds. Upper right: solar insolation in WRF using GOES insolation values. Lower panel: differences in insolation values.

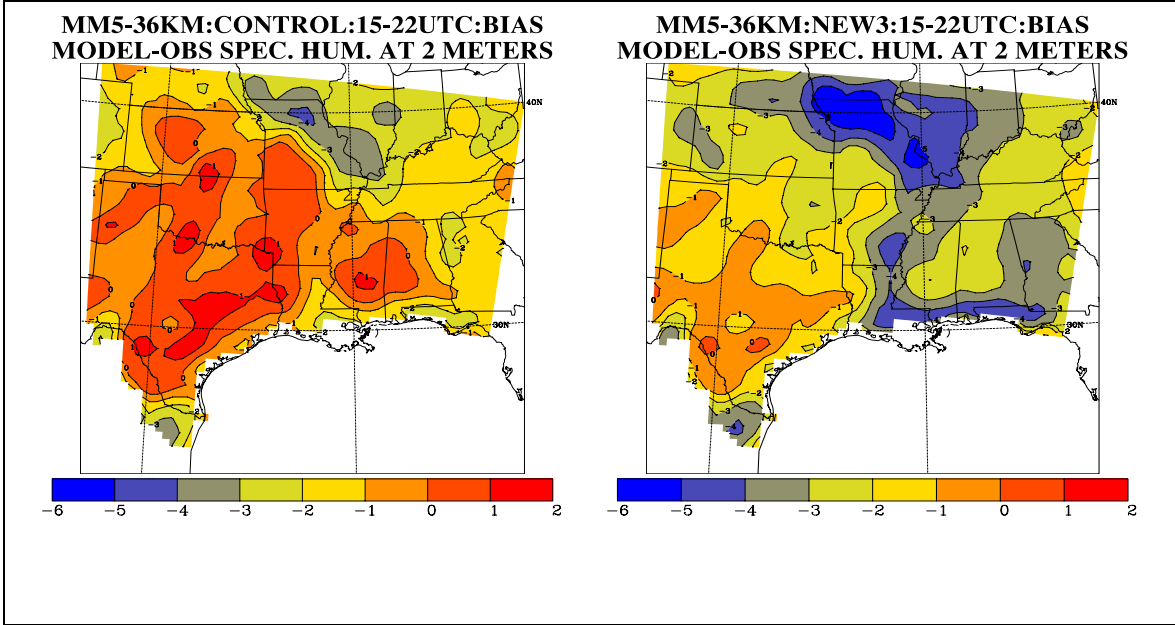


Figure 18. Comparison of model specific humidity show with NWS observed specific humidity (derived from dew point temperatures). The results show that the benchmark or control case (left panel) shows that the model is too moist. The case with the satellite adjustment (right panel) shows that the model has actually over-dried the atmosphere.